The International Journal of Advanced Manufacturing Technology (2022) 123:407–430
https://doi.org/10.1007/s00170-022-10160-z

ORIGINAL ARTICLE

Modeling and optimization of machining parameters to minimize surface roughness and maximize productivity when turning polytetrafluoroethylene (PTFE)

Afef Azzi[1,2] · Lakhdar Boulanouar[1] · Aissa Laouisi[3] · Alima Mebrek[2] · Mohamed Athmane Yallese[3]

Received: 21 June 2022 / Accepted: 14 September 2022 / Published online: 28 September 2022

Abstract

The objective of this work is to study the impact of the machining parameters (*ap*, *f*, and *Vc*) on the technological parameters, surface roughness criteria (Ra, Rz), and material removal rate (MRR) during the turning of polytetrafluoroethylene (PTFE) polymer. The machining tests were carried out using a square metal carbide insert in compliance with the Taguchi design (L27). ANOVA was used to determine the influence and contribution of machining parameters (*ap*, *f*, and *Vc*) on the output parameters (*Ra*, *Rz*, and *MRR*). It was indicated that the surface roughness and the material removal rate are strongly affected by the feed rate with contributions of 90.02, 91.81, and 49.22% for *Ra*, *Rz*, and *MRR*, respectively. The response surface methodology (RSM) and the artificial neural networks (ANN) approach were used for output technological parameter modeling to discern the most efficient one. Finally, the desirability function (DF) was used to determine optimal cutting parameters. The optimization was carried out using three approaches, which are quality, productivity, and the combination of quality and productivity. The results showed that the optimal parameters for minimizing roughness and maximizing MRR were found as ap = 2 mm, *f* = 0.126 mm/rev, and Vc = 270 m/min.

Keywords Machining · PTFE · Surface roughness · ANOVA · RSM · ANN · Modeling · Optimization

Abbreviations

ANOVA	Analysis of variance
ANN	Artificial neural network
RSM	Response surface methodology
ap	Depth of cut (mm)
Vc	Cutting speed (m/min)
f	Feed rate (mm/rev)
cont %	Contribution ratio (%)
DF	Desirability function
F value,	Ratio of mean square of regression model
R^2	Determination coefficient
Ra	Arithmetic mean roughness (µm)
Rz	Mean depth of roughness (µm)
MRR	Material removal rate (cm^3/min)
SS	Sequential sum of squares
SC	Sum of squares

✉ Afef Azzi
a.azzi@crti.dz; afef.azzi@yahoo.fr

[1] Research Laboratory of Advanced Technologies in Mechanical Production "LRTAPM," Department of Mechanical Engineering, Badji Mokhtar University, BP 12, 23000 Annaba, Algeria

[2] Research Centre in Industrial Technologies (CRTI), PO Box 64, Cheraga, 160141 Algiers, Algeria

[3] Structures and Mechanics Laboratory (LMS), Mechanical Engineering Department, May 8th, 1945 University, PO Box 401, 24000 Guelma, Algeria

1 Introduction

Over the last decade, polymer machining has been developed as an alternative to injection molding, sintering, or extrusion processes. This is due to the need for cost-effective manufacturing methods when using high-performance polymeric materials with higher mechanical and thermal properties. One of the best thermoplastic polymers is polytetrafluoroethylene (PTFE), a semi-crystalline, soft, easily definable, opaque, and white material, and its trade name is "Teflon." PTFE is a remarkable material in many functions [1], due to its excellent mechanical properties with a low coefficient of friction [2], thermal insulation [3, 4], and dielectric [5]. The PTFE cylindrical bars have played an essential role in the industry, which are widely used in the aeronautical field, containers for reactive chemicals, seals, coatings, electrical

insulation, kitchen utensils, manufacturing gears, pinions, bearings [1, 6], medical, and biotechnology applications [7]. Optimization of turning parameters to achieve a quality set of attributes for productivity needs at an economical cost, superior material removal rate, and good surface finish are the main goals of the turning process on PTFE [8]. Surface roughness is an important characteristic in industrial applications and includes friction, lubrication, heat transfer, corrosion resistance, and wear. Surface roughness is a crucial element in manufacturing applications that determines the reliability and longevity of the parts [9, 10].

The better machinability and better product efficiency offer low surface roughness levels [2]. Mohd et al. [11] conducted the study experiments on cutting force and roughness in the turning of bronze reinforced polymer (PTFE). They noted that the cutting parameters, which give the best results, are as follows: $ap = 0.5$ mm, la $f = 0.05$, and $Vc = 100$ m / min.

Kaladhar et al. [12] have used the Taguchi method for surface roughness optimization and tool flank wear in turning of AISI 4340 steel (35 HRC). ANOVA found that the cutting speed is the most, $f = 0.15$ mm/rev and $ap = 0.25$ mm.

Fetecau and Stan [13]. studied the effect of the cutting force and roughness in the turning of polytetrafluoroethylene (PTFE) composites with a polycrystalline diamond tool. The statistical results indicate that the cutting force is significantly influenced (at 95% confidence level) by feed rate, depth of cut, and the interaction of the feed rate with a depth of cut, while the cutting speed and insertion radius have a minor influence. The cutting force increases with increasing feed rate and depth of cut, respectively.

A prediction model based on ANN was developed to determine the optimum cutting parameters in surface roughness terms for the turning of 25% glass fiber-filled PTFE and 25% carbon-filled. The experimental results were compared with the ANN model performance in order to determine its effectiveness; Sanci et al. performed it [2].

Sanjeev Kumar et al. [14] have studied optimizing the best machining parameters of polytetrafluoroethylene (PTFE) and minimizing roughness. They found that the optimal roughness was ($Ra = 61.92$ µm) using the genetic algorithm in the 9th generation, cutting speed = 158.06 m/min, feed rate = 0.16 mm/rev, and the depth of cut = 1.719 mm. These results present the best parameters to obtain a minimum surface roughness in the machining of PTFE tubes to improve the airflow in aircraft and aircraft air conditioning systems.

Chabbi et al. [15] used both Taguchi analysis, RSM, ANN, and DF methods when studying the influence of machining parameters during the turning of polymer polyoxymethylene (POM C). They investigated the influence of surface roughness (Ra), cutting force (Fz), cutting power (Pc), and the material removal rate (MRR). They concluded that the feed rate presents the most important in surface roughness and the depth of cut presents the most influential parameter on (Pc) and (Fz).

Subramanian et al. [16] have used the ANOVA methodology for surface roughness optimization in the turning cylindrical Teflon rods (PTFE).

Anand et al. [17] carried out the machining parameter optimization during the drilling of polymeric nano-composites using ANN models, fuzzy logic, and gray relational analysis (GRA). They revealed that the drill diameter exhibits the most important factor, followed by the feed rate and the spindle speed.

Azizi et al. [18] have studied the effect of the cutting parameters on the surface roughness, the radial tool vibration, and the stock removal rate with a turning hard EN19 alloy steel in dry conditions and using the response surface methodology (RSM). They reported that the multi-objective optimization is $Vc = 95.2$ m/min, $f = 0.125$ mm/rev, $ap = 1.2$ mm with estimated surface roughness $Ra = 0.925$ µm, tool radial vibration $Vy = 0.499$ mm/s, and material removal rate $MRR = 14.5$ cm^3/min.

Literature is prolific and widely available in the field of machining metallic materials and alloys, but there are fewer academic papers on polymer machining. There is very limited literature in this field, especially the machining of PTFE.

The purpose of the present experimental investigation is to determine the impact and optimization of the machining parameters such as (ap, f, and Vc) on surface roughness (Ra, Rz) and material removal rate (MRR) when turning polytetrafluoroethylene (PTFE). The response surface methodology and the artificial neural network method are used to develop mathematical prediction models. A comparative analysis of roughness criteria (Ra, Rz) was carried out between both methods in terms of the R^2, MAPE, and MAD to determine the most effective. Finally, the desirability function (DF) was used to find optimal machining parameters. According to three desired cases; minimizing (Ra), maximizing (MRR), and compromising between (Ra, Rz) and (MRR).

2 Experimental

2.1 Materials and equipment

The used material in this study is a Teflon (PTFE) with a diameter of 90 mm and several levels of 20 mm long, separated by grooves of 2 mm. The machining was done on a TOS TRENCIN lathe model SN40 with a spindle power of 6.6 KW. The tests were conducted using a square plate metal carbide of the shade SCMM120512T (P30) designation. The insert was mounted on the tool holder of the CSDPN2525M12 designation with a positive rake angle.

The roughness measurement (Ra, Rz) was performed with a surf test roughness meter (Mitutoyo) model 201. For more precision, the roughness tests were performed directly on the machine tool for each test (L_{27}); the experimental setup will be seen in Fig. 1.

Table 1 Levels of the different machining parameters

Level	*ap (mm)*	*f (mm/rev)*	*Vc (m/min)*
1	1	0.08	135
2	1.5	0.16	190
3	2	0.24	270

2.2 Experimental design

Taguchi L_{27} plan is applied for the experiment planning to develop the mathematical models necessary for this study. The selected input factors (*ap*, *f*, and *Vc*), and the levels are grouped in Table 1.

The material removal rate (MRR) is defined as the quantity of material extracted per unit of time, specifically aimed at process productivity. This needs to be maximized in roughing operations [19]. MRR is calculated with the obtained results, as follows in Eq. (1):

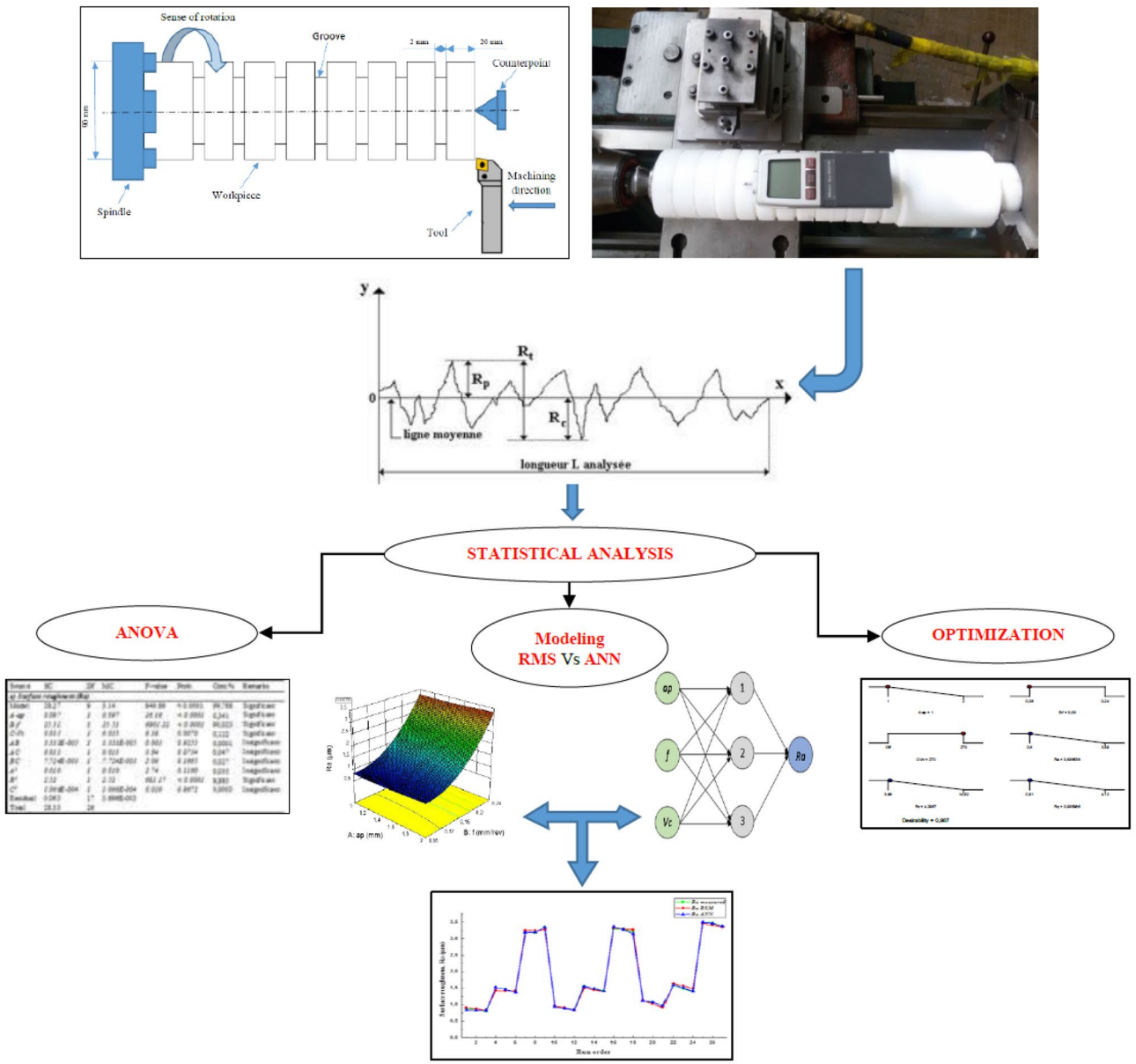

Fig. 1 Experimental setup of the experimental procedure and methodology

$$\mathrm{MRR} = \mathrm{ap} \times f \times \mathrm{Vc} \quad (1)$$

3 Results and discussion

Table 2 presents the coded factors, machining parameters (ap, *f*, and Vc), and the response factors Ra, Rz, and MRR according to the factorial design L_{27}. It can be seen that the arithmetic mean roughness (Ra) was obtained in the range of 0.8–3.49 µm, the profile maximum height (Rz) was obtained in the range of 3.98–14.92 µm, and the calculation of the material removal rate MRR varies between 10.8 and 129.6 (cm^3/min).

3.1 Statistical analysis

3.1.1 Analysis of variance (ANOVA)

The ANOVA results for surface roughness (*Ra*) were given in Table 3 part a. We can say that the feed rate (*f*) is the most important factor, which influences the surface roughness (Ra), followed by the product (f^2) which have contributions of 90.02 and 8.88%, respectively. Cutting speed (*Vc*) and depth of cut (*ap*) have statistically significant effects of less than 1%, while the products (V^2, ap^2) and interactions (*Vc*×*f, Vc*×*ap and f*×*ap*) have no significant intensity.

The analysis presented in Table 3 part b shows that the feed rate (*f*) is the most important factor, which influences the surface roughness (*Rz*). Its contribution is 91.81%, *Vc* with 1.32% contribution. The depth of cut (*ap*) is not significant in the surface roughness (Rz); however, the factor (f^2) has a contribution of 5.67%, and the other factors are not significant. Table 3 part c illustrates the ANOVA results for material removal rate (MRR). One observes also that the feed rate (*f*) presents the most important factor with a contribution of 49.22%, followed by *Vc* and *ap* with contributions of 22.00 and 21.87%, respectively. The interactions (ap×*f*, *ap*×*Vc*, and *f*×Vc) are less important and vary between 1.64 and 3.70%. To conclude, ANOVA revealed that the feed rate is a more significant factor than the surface roughness

Table 2 Experimental results for Ra, Rz, and MRR

Run	Coded factors			Actual factors			Response variables		
	A	*B*	*C*	*ap (mm)*	*f (mm/rev)*	*Vc (m/min)*	*Ra (µm)*	*Rz (µm)*	MRR (cm^3/min)
1	−1	−1	−1	1	0.08	135	0.89	5.32	10.8
2	−1	−1	0	1	0.08	190	0.86	4.93	15.2
3	−1	−1	+1	1	0.08	270	0.8	4.72	21.6
4	−1	0	−1	1	0.16	135	1.51	8.7	21.6
5	−1	0	0	1	0.16	190	1.46	7.19	30.4
6	−1	0	+1	1	0.16	270	1.4	6.3	43.2
7	−1	+1	−1	1	0.24	135	3.18	14.66	32.4
8	−1	+1	0	1	0.24	190	3.19	13.99	45.6
9	−1	+1	+1	1	0.24	270	3.34	13.73	64.8
10	0	−1	−1	1.5	0.08	135	0.94	5.19	16.2
11	0	−1	0	1.5	0.08	190	0.9	5.04	22.8
12	0	−1	+1	1.5	0.08	270	0.84	4.62	32.4
13	0	0	−1	1.5	0.16	135	1.56	8.5	32.4
14	0	0	0	1.5	0.16	190	1.48	7.14	45.6
15	0	0	+1	1.5	0.16	270	1.42	6.98	64.8
16	0	+1	−1	1.5	0.24	135	3.3	14.92	48.6
17	0	+1	0	1.5	0.24	190	3.28	14.67	68.4
18	0	+1	+1	1.5	0.24	270	3.22	13.74	97.2
19	+1	−1	−1	2	0.08	135	1.12	5.29	21.6
20	+1	−1	0	2	0.08	190	1.07	4.58	30.4
21	+1	−1	+1	2	0.08	270	0.98	3.98	43.2
22	+1	0	−1	2	0.16	135	1.58	8.31	43.2
23	+1	0	0	2	0.16	190	1.49	7.25	60.8
24	+1	0	+1	2	0.16	270	1.4	7.23	86.4
25	+1	+1	−1	2	0.24	135	3.49	14.16	64.8
26	+1	+1	0	2	0.24	190	3.48	13.97	91.2
27	+1	+1	+1	2	0.24	270	3.38	13.71	129.6

Table 3 Analysis of variance for (a) *Ra*, (b) *Rz*, and (c) *MRR*

Source	SC	Df	MC	*F* value	Prob.	Cont.%	Remarks
(a) Surface roughness (Ra)							
Model	28.27	9	3.14	849.89	< 0.0001	99.788	Significant
A-ap	*0.097*	*1*	*0.097*	*26.16*	*< 0.0001*	0.341	Significant
B-f	*25.51*	*1*	*25.51*	*6901.22*	*< 0.0001*	90.023	Significant
C-Vc	*0.035*	*1*	*0.035*	*9.38*	*0.0070*	0.122	Significant
AB	*3.333E-005*	*1*	*3.333E-005*	*0.003*	*0.9255*	0.0001	Insignificant
AC	*0.013*	*1*	*0.013*	*3.64*	*0.0734*	0.047	Insignificant
BC	*7.724E-003*	*1*	*7.724E-003*	*2.09*	*0.1665*	0.027	Insignificant
A^2	*0.010*	*1*	*0.010*	*2.74*	*0.1160*	0.035	Insignificant
B^2	*2.52*	*1*	*2.52*	*681.17*	*< 0.0001*	8.885	Significant
C^2	*1.066E-004*	*1*	*1.066E-004*	*0.029*	*0.8672*	0.0003	Insignificant
Residual	0.063	17	3.696E-003				
Total	28.33	26					
(b) Surface roughness (Rz)							
Model	421.05	9	46.78	360.02	< 0.0001	99.478	Significant
A-ap	*0.051*	*1*	*0.051*	*0.39*	*0.5393*	0.012	Insignificant
B-f	*388.60*	*1*	*388.60*	*2990.39*	*< 0.0001*	91.810	Significant
C-Vc	*5.60*	*1*	*5.60*	*43.09*	*< 0.0001*	1.323	Significant
AB	*0.028*	*1*	*0.028*	*0.22*	*0.6482*	0.006	Insignificant
AC	*0.096*	*1*	*0.096*	*0.74*	*0.4009*	0.022	Insignificant
BC	*8.609E-004*	*1*	*8.609E-004*	*0.003*	*0.9361*	0.000	Insignificant
A^2	*0.24*	*1*	*0.24*	*1.83*	*0.1943*	0.056	Insignificant
B^2	*24.03*	*1*	*24.03*	*184.89*	*< 0.0001*	5.676	Significant
C^2	*0.35*	*1*	*0.35*	*2.73*	*0.1170*	0.083	Insignificant
Residual	2.21	17	0.13				
Total	423.26	26					
(c) Material removal rate ***(MRR)***							
Model	21410.85	9	2378.98	685.62	< 0.0001	99.73	Significant
A-ap	4697.38	1	4697.38	1353.79	< 0.0001	21.878	Significant
B-f	10569.09	1	10569.09	3046.02	< 0.0001	49.227	Significant
C-Vc	4723.92	1	4723.92	1361.44	< 0.0001	22.002	Significant
AB	755.25	1	755.25	217.66	< 0.0001	3.517	Significant
AC	353.92	1	353.92	102.00	< 0.0001	1.648	Significant
BC	796.32	1	796.32	229.50	< 0.0001	3.709	Significant
A^2	0.000	1	0.000	0.000	1.0000	0.000	Insignificant
B^2	0.000	1	0.000	0.000	1.0000	0.000	Insignificant
C^2	0.000	1	0.000	0.000	1.0000	0.000	Insignificant
Residual	58.99	17	3.47				
Total	21469.84	26					

(Ra and Rz) and the material removal rate MRR with the contributions of 90.02, 91.81, and 49.22%, respectively.

The Pareto charts (Fig. 2) have classified the machining parameters and their correlations from the largest effect to the smaller effect, according to their corresponding Fisher's test values (*F* value) at 95% ($\alpha = 0.05$) confidence level. Standard values in Fig. 2 are calculated by dividing the mean square of each factor by the error mean square, if the *F* values for the surface roughness criteria Ra, Rz, and the material removal rate (MRR) are greater than 2.11 which is noteworthy that it is depicted as a red line of color which are important (significant). Based on the results of the variance analysis (Table 3) and the Pareto diagram (Fig. 2), it can be deduced that the feed rate is the most important parameter influencing the surface roughness and the material removal rate. Therefore, the results of ANOVA (Ra, Rz, and MRR) are confirmed by the Pareto chart.

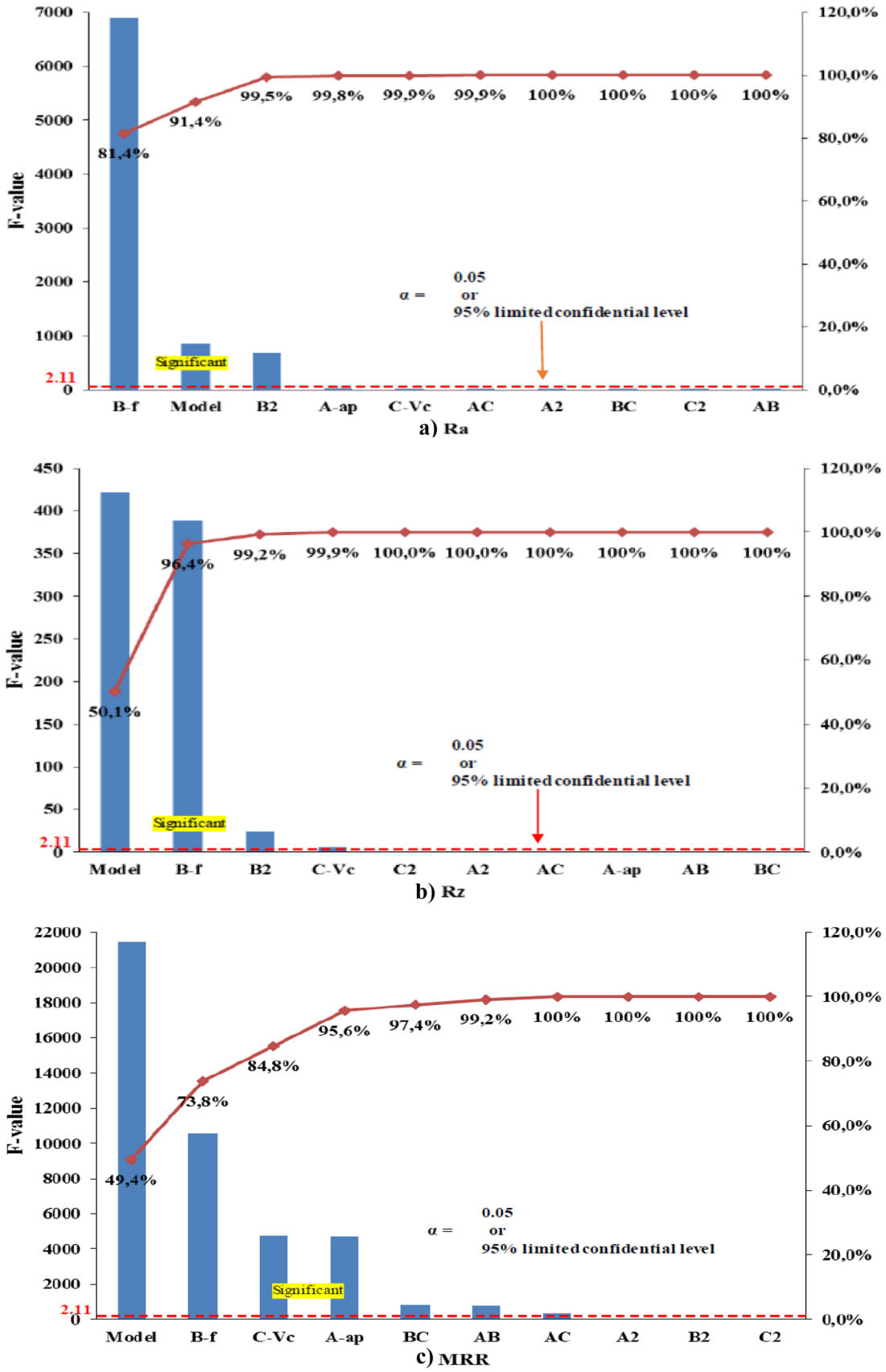

Fig. 2 Results of Pareto charts of surface roughness: **a** Ra, **b** Rz, and **c** MRR

4 Modeling of cutting parameters

4.1 Response surface methodology RSM

The relationship between depth of cut (*ap*), feed rate (*f*), and cutting speed (*Vc*) and the outputs titled *Y* defines the machinability of polytetrafluoroethylene (PTFE) in terms of (*Ra*, *Rz*, and *MRR*), and this rapport is given by Eq. (2):

$$Y = K(Vc, f, ap) + e_{ij} \tag{2}$$

where *Y* is the desired machinability aspect and *K* is a function proposed by using a non-linear quadratic mathematical model, which is suitable for studying the interaction effects of process parameters on machinability characteristics.

In the present work, the mathematical model of the second-order based on RSM (Eq. (3)) was calculated using Design-Expert version 10 software:

$$\begin{aligned} \mathrm{Y} = {} & \mathrm{a_0} + \mathrm{a_1A} + \mathrm{a_2B} + \mathrm{a_3C} + \mathrm{a_{12}AB} + \mathrm{a_{13}AC} \\ & + \mathrm{a_{23}BC} + \mathrm{a_{11}A^2} + \mathrm{a_{22}B^2} + \mathrm{a_{33}C^2} \end{aligned} \tag{3}$$

where a_o is constant; a_1, a_2, a_3, and a_{11}, a_{22}, and a_{33} represent the coefficients of linear quadratic; and a_{12}, a_{13}, and a_{23} represent the interactions terms, respectively. *A*, *B*, and *C* reveal the coded variables that correspond to the studied machining parameters.

The coded variables *A*, *B*, and *C* are obtained from the following transformation equations:

$$A = \frac{ap - apo}{\Delta ap} \tag{4}$$

$$B = \frac{f - fo}{\Delta f} \tag{5}$$

$$C = \frac{Vc - Vco}{\Delta Vc} \tag{6}$$

where:

A, *B*, and *C* are the coded values of parameters *ap*, *f*, and *Vc*, respectively.

ap_o, f_o, and Vc_o are factors at zero level.

Δap, Δf, and ΔVc are the increment values of *ap*, *f*, and *Vc*, respectively.

Many researchers used the response surface methodology RSM to estimate the influence of input parameters on the response factors and to create predictive mathematical models and plots 3D of the response surface [15, 20–23]. The arithmetic means roughness (Ra), the maximum height of the profile (Rz), the material removal rate (MRR), and its coefficients of determination (experimental and adjusted) are given in Eqs. (7)–(9):

$$\begin{aligned} Ra = {} & 1.83054 - 0.15319ap - 18.47512f - 3.07687Vc + 0.041667ap \times f \\ & - 9.86739 \times 10^{-4} ap \times Vc + 4.67149 \times 10^{-3} f \times Vc + 0.16444ap^2 \\ & + 101.21528f^2 + 9.63337 \times 10^{-7} Vc^2 (R^2 = 99.78\%, R^2{}_{adj} = 99.66\%) \end{aligned} \tag{7}$$

$$\begin{aligned} Rz = {} & 9.48615 + 1.55169ap - 43.30872f - 0.034472Vc + 1.20833ap \times f \\ & + 2.64135 \times 10^{-3} ap \times Vc - 1.55967 \times 10^{-3} f \times Vc - 0.79556ap^2 \\ & + 312.67361f^2 + 5.55462 \times 10^{-5} Vc2 (R^2 = 99.48\%, R^2{}_{adj} = 99.20\%) \end{aligned} \tag{8}$$

$$\begin{aligned} MRR = {} & 47.6 - 31.73 \times ap - 297.5 \times f - 0.240 \times Vc - 0.00 \times ap^2 - 0.00f^2 \\ & + 0.00Vc^2 + 198.3 \times ap \times f + 0{,}160 \times ap \times Vc + 1.500 \times f \times Vc \\ & (R^2 = 99.73\%, R^2{}_{adj} = 99.58\%) \end{aligned} \tag{9}$$

To reduce the models, only the significant parameters will be conserved and are given by Eqs. (10) to (12):

$$Ra = 1.58598 + 0.15111\ ap - 17.48611f - 6.46373Vc + 101.21528\, f^2 \tag{10}$$

$$Rz = 7.79063 - 41.80556f - 8.04240Vc + 312.67361\, f^2 \tag{11}$$

$$\begin{aligned} MRR = {} & 47.600 - 31.733 \times ap - 297.500 \times f - 0.240 \times Vc \\ & + 198.333 \times ap \times f + 0.160 \times ap \times Vc + 1.500 \times f \times Vc \end{aligned} \tag{12}$$

The coefficients of determination values R^2 for the components of the roughness criteria (Ra, Rz) and the material removal rate (MRR) models are, respectively, $R^2 = 0.9778$, $R^2 = 0.9948$, and $R^2 = 0.9973$.These values indicate that the developed models explain 99.78, 99.48, and 99.73% of the variation (Ra, Rz, and MRR). The surface roughness (Ra, Rz) and the material removal rate MRR of the adjusted coefficient value of the model determination are, respectively, 99.66, 99.20, and 99.58%. They represent a correction of R^2, which takes into account the number of variables used in the model. These two values of the determination coefficients R^2 and R^2_{adj} show a very good correlation between the values predicted by this model, and the results measured experimentally are higher and suggest great importance of the models and display a good agreement with the experimental data.

Figure 3a–c shows a comparison between the values estimated by the developed model deduced from the (Ra, Rz, and MRR) and the experimental values obtained. The previous models can be used to predict the surface roughness (Ra, Rz), and the material removal rate MRR, for the selected cutting conditions. These figures indicate that the quadratic models are capable of the system representing in the given experimental domain. The comparison results illustrate that the predicted values of the studied technological parameters are closer to the experimental values.

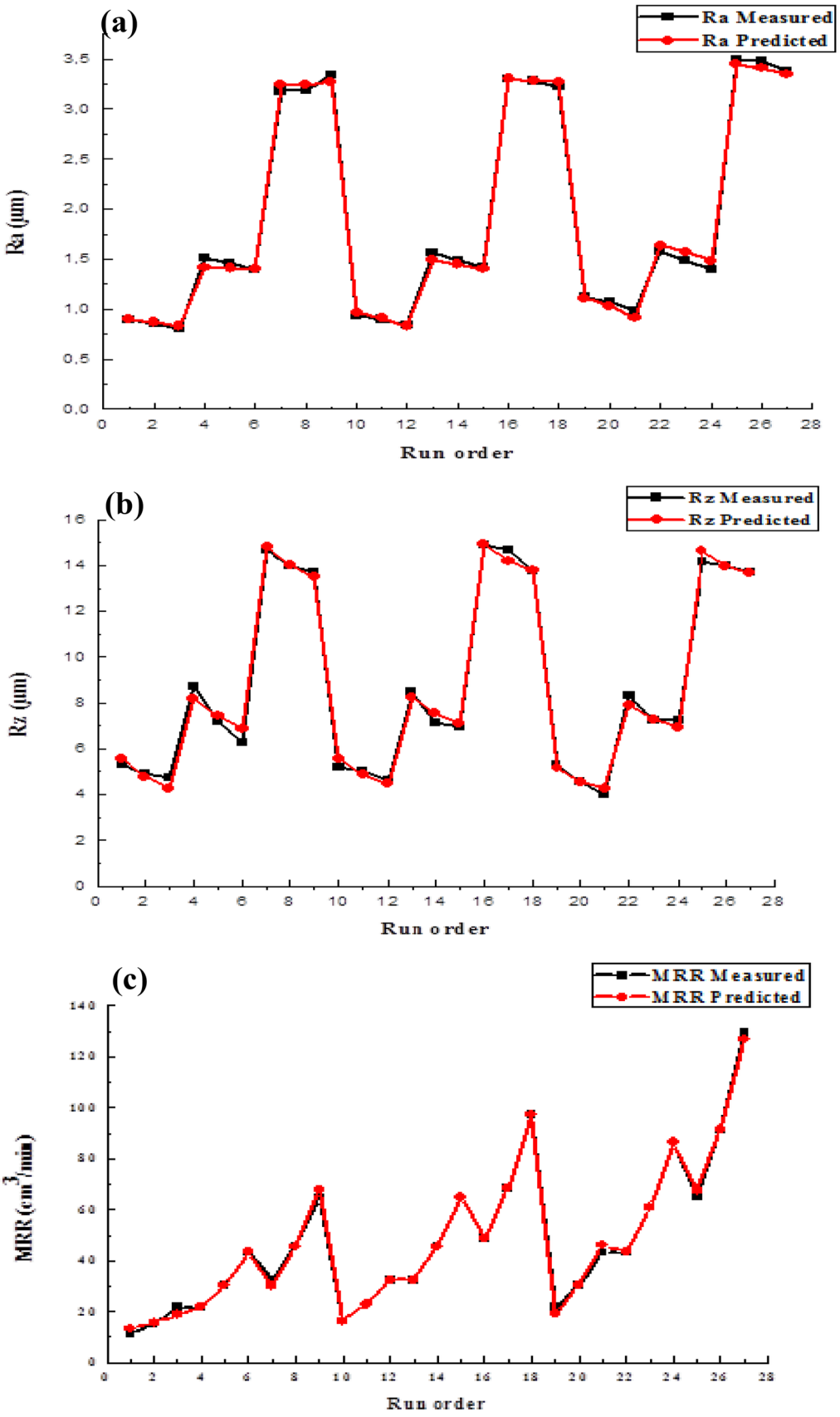

Fig. 3 Comparison results of predicted and measured **a** Ra, **b** Rz, and **c** MRR

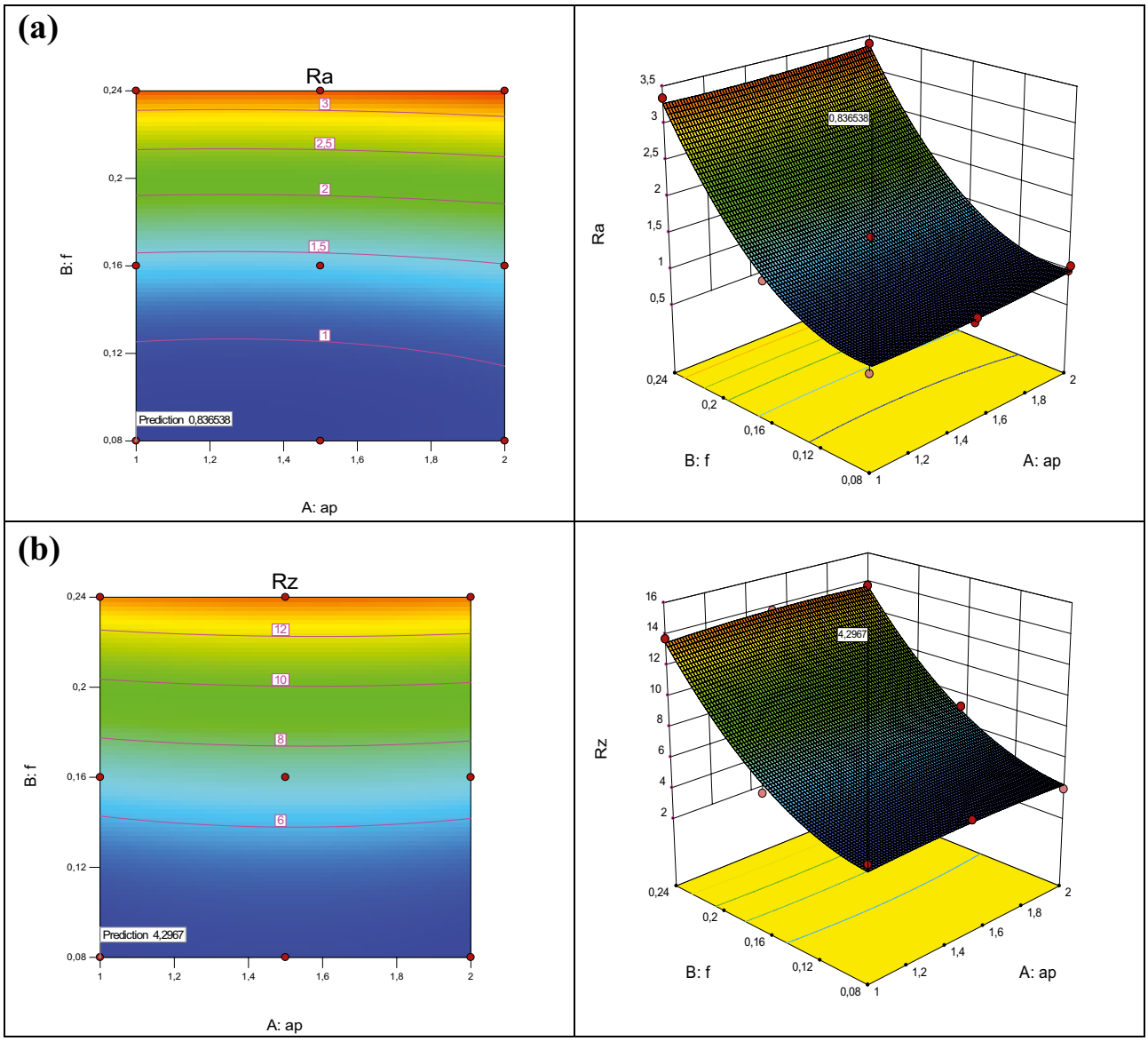

Fig. 4 Effect of depth of cut and feed rate on surface roughness parameters at Vc = 270 m/min, **a** Ra and **b** Rz

To visualize the influence of the cutting parameters on the surface roughness (Ra, Rz), and the material removal rate (MRR), the response surfaces (3D), and the contour graphics were plotted based on Eqs. (7)–(9) of the model quadratic shown in Figs. 4, 5 and 6. Each model allowed three variables (*ap*, *f*, and *Vc*), and one of the variables was kept constant at the central level for each plot; therefore, a total of three response area plots were created from the responses (Figs. 4, 5 and 6). The influence of the feed rate (*f*) and the depth of cut (*ap*) on the surface roughness (*Ra*) with a constant cutting speed are presented in Fig. 4. It is observed that the surface roughness increases rapidly with increasing feed rate; however, the depth of cut does not have a significant effect on the surface roughness criteria. Figure 5 illustrates the interaction effect between the feed rate (*f*) and the cutting speed (*Vc*) on the surface roughness while maintaining the depth of cut (*ap*) at a constant level. It is noted that the surface roughness increases with increasing feed rate; however, the cutting speed shows no significant change in the surface quality. This suggests that the feed rate effect is the main significant factor contributing to the surface roughness variation. In conclusion, the interaction effects between the cutting speed (*Vc*) and the depth of cut (*ap*) on the surface roughness criteria (*Ra*, *Rz*) are shown in Fig. 6. One demonstrated that the cutting speed increasing and depth of cut have negligible effects on the surface roughness.

It revealed that a combination of higher cutting speed along with a lower feed rate and depth of cut is necessary for minimizing the surface roughness. A surface finish improvement Ra of 0.837 µm and Rz of 4.297 µm was recorded with

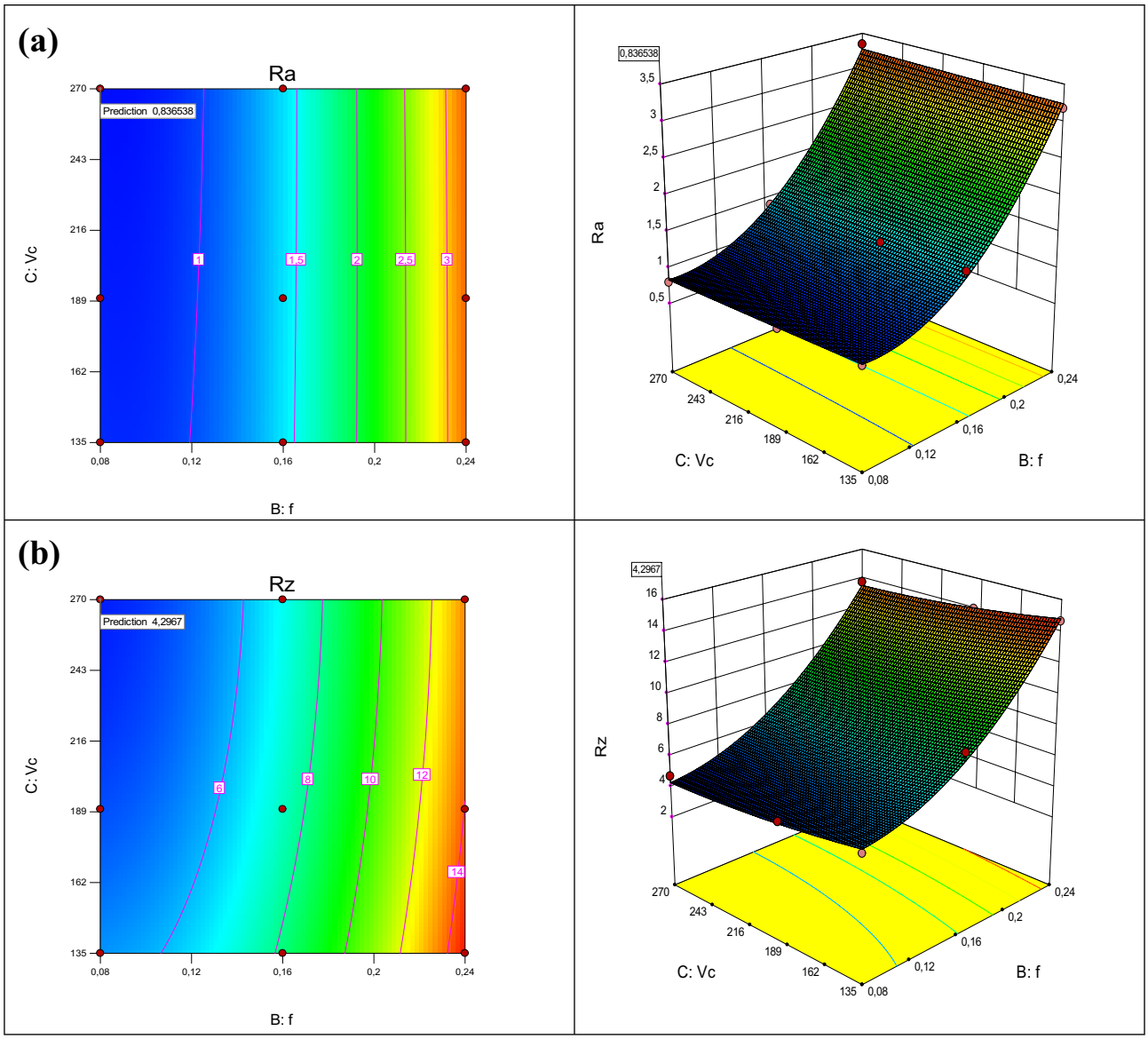

Fig. 5 Effect of feed rate and cutting speed on surface roughness parameters at ap = 1 mm, **a** Ra and **b** Rz

a depth of cut of 1 mm, feed rate of 0.08 mm/rev, and at a higher cutting speed of 270 m/min.

Figure 7 illustrates the 3D plots of the (MRR) on a function of the combination of cutting parameters (*Vc*, *f*, and *ap*). It should be noted that the increase of the three values of (*Vc*, *f*, and *ap*) increases the maximal material removal rate (Eq. (1)).

4.2 Artificial neural network ANN

Artificial neural network (ANN) is potentially more accurate [24] and one of the best known predictive models which are capable to estimate the output parameter of the machining process in the range of input parameters studied. Several researchers have used ANNs for modeling the turning process successfully [25–27]. A neuron or node is classified as a single processor for junction measurements and transfer functions. In addition, and according to Hagan et al. research [28], the transmitted information between neurons was defined by the difference in weight (w) and biases (b). The increasing success of neural networks over other statistical technics can be due to their strength, flexibility, and ease of use [29].

In this study, a prediction model based on ANN was developed to determine the optimum cutting parameters (depth of cut, feed rate, and cutting speed) as a function of the surface roughness (Ra, Rz) in the turning of PTFE. The performance of the ANN model was compared with experimental results to determine its effectiveness. The ANN model is generally represented graphically as given

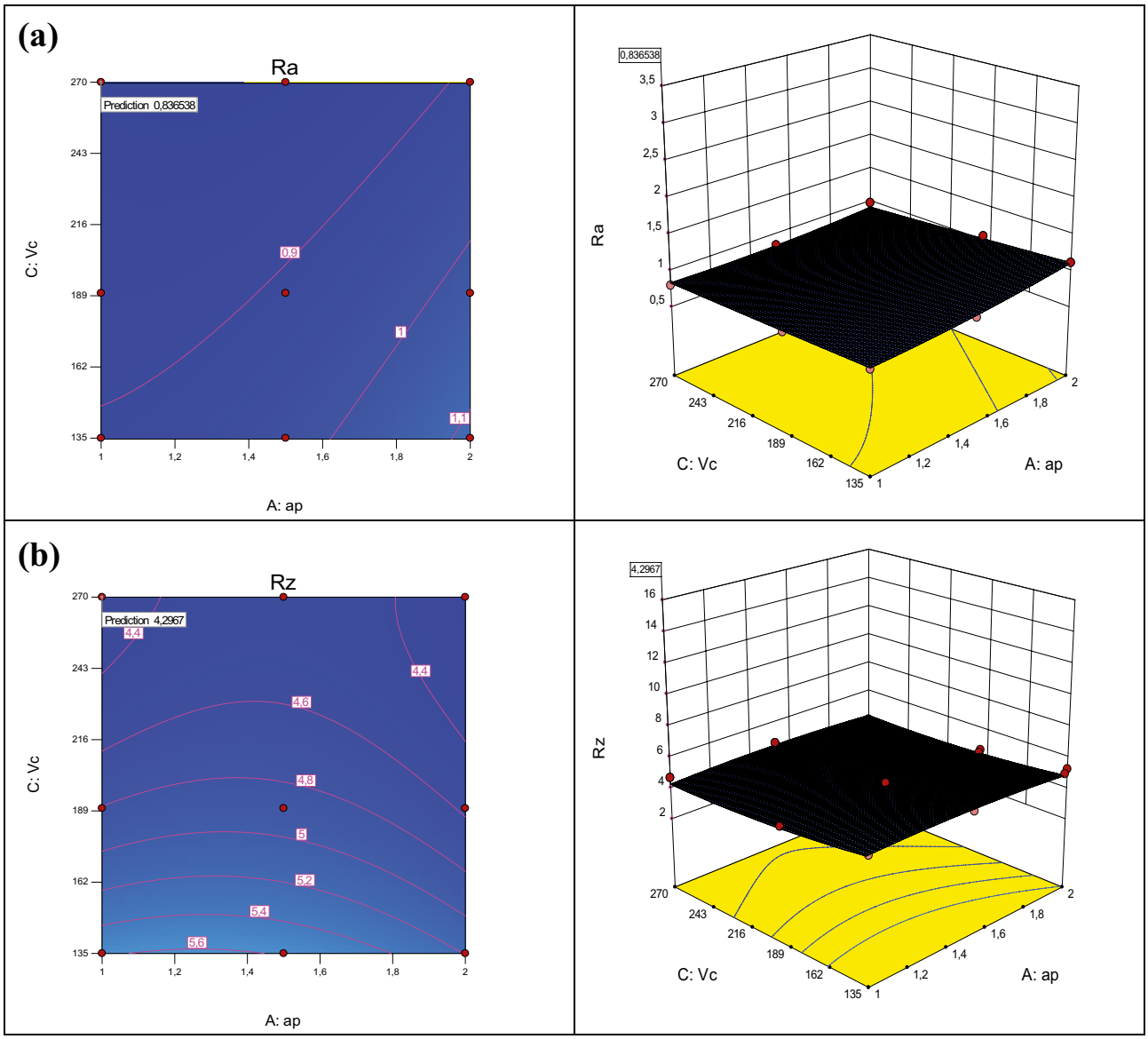

Fig. 6 Effect of depth of cut and cutting speed on surface roughness parameters at $f = 0.08$ mm/rev, **a** Ra and **b** Rz

in Fig. 8. The surface roughness Ra and Rz they modeled separately, with three hidden neurons (nodes) for each. The neuron number in the input layer is fixed as three neurons (ap, *f*, and Vc). The output layer contains a single neuron, which indicates the desired response (Ra, Rz, and MRR). The activation function used is a hyperbolic tangent (TanH) with a sigmoid function (Eq. (13)), which transforms the values between (−1 and 1). *x* is the linear combination of the *X* variables [30]. The general graph of the opted neural network for the surface roughness is illustrated in Fig. 9:

$$TanH = \frac{e^{2x} - 1}{e^{2x} + 1} \tag{13}$$

The ANN models of the surface roughness (Ra, Rz) and the material removal rate (MRR) have been written as follows:

$$\begin{aligned} Ra = {} & 4.4398 + 0.0392 \times H1 + 0.19259 \times H2 + 5.8890 \\ & \times H3 + 0.6183 \times H4 + 0.1514 \times H5 + 0.5205 \times H6 + 0.7458 \\ & \times H7 - 0.0787 \times H8 + 1.0465 \times H9 - 2.2093 \times H10 \end{aligned} \tag{14}$$

$$\begin{aligned} Rz = {} & 17.2032 + 3.8599 \times H1 + 1.6810 \times H2 + 18.5586 \\ & \times H3 + 0.7131 \times H4 + 0.1207 \times H5 - 0.1866 \times H6 + 3.8563 \\ & \times H7 + 2.1838 \times H8 + 5.6968 \times H9 - 5.1926 \times H10 \end{aligned} \tag{15}$$

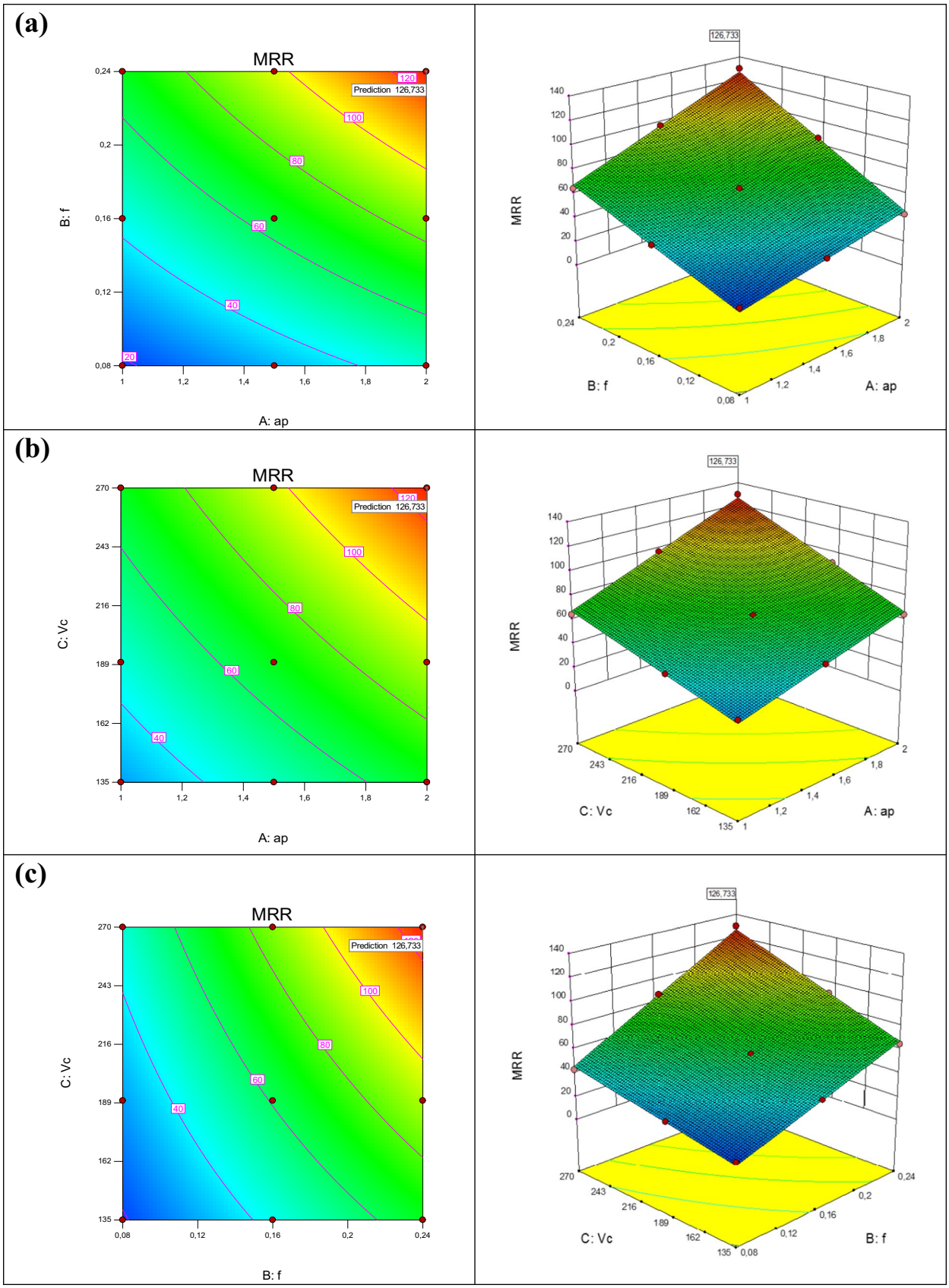

Fig. 7 Estimated response surface for MRR depending on: **a** ap, **b** *f*, and **c** Vc

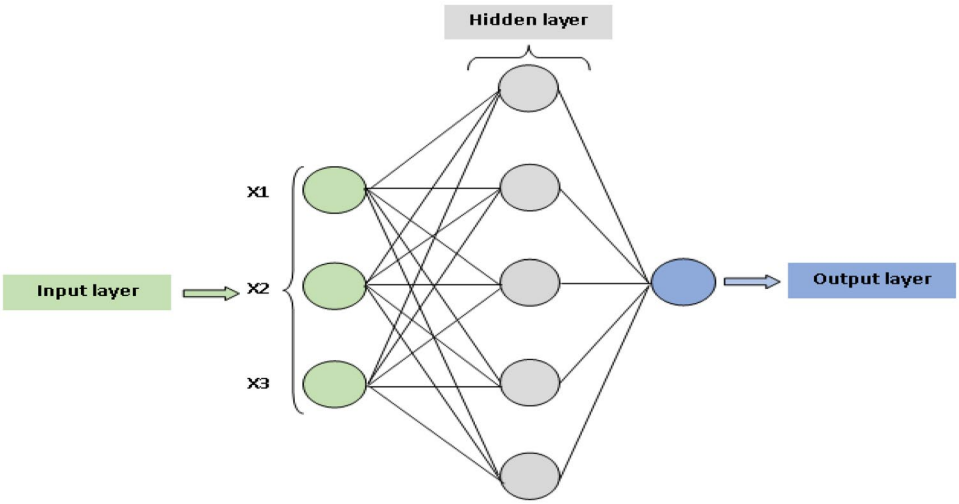

Fig. 8 The ANN general graph

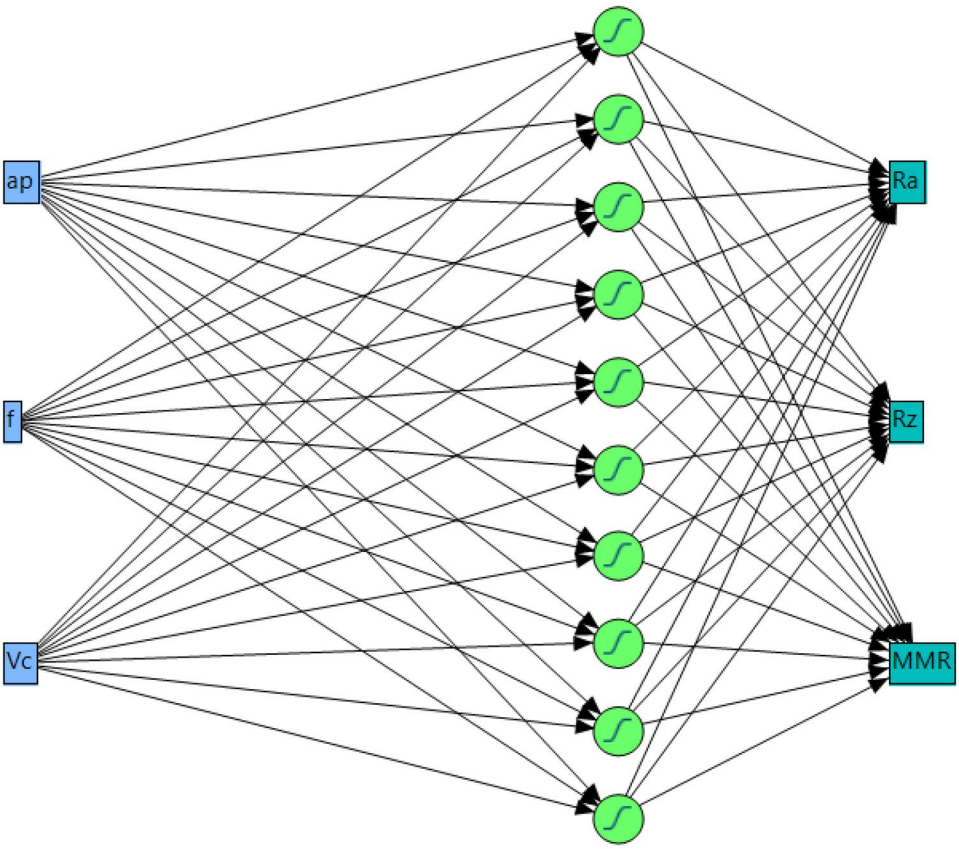

Fig. 9 Neural network architecture chosen for Ra, Rz, and MRR

$$\begin{aligned} \mathrm{MMR} = {} & 43.2727 + 42.2353 \times \mathrm{H1} - 2.9719 \times \mathrm{H2} + 39.4888 \\ & \times \mathrm{H3} - 24.4053 \times \mathrm{H4} + 22.2320 \times \mathrm{H5} - 41.2604 \times \mathrm{H6} - 66.7335 \\ & \times \mathrm{H7} + 19.4229 \times \mathrm{H8} - 47.6191 \times \mathrm{H9} + 18.3143 \times \mathrm{H10} \end{aligned} \tag{16}$$

With:

$$\mathrm{H1} = \mathrm{TanH}\,(0.5 \times (-4.6886 + 0.8855 \times \mathrm{ap} + 7.2974 \times f + 0.0077 \times \mathrm{Vc}))$$

$$H2 = \tanh(0.5 \times (3.4588 + 0.9032 \times ap - 15.9704 \times f - 0.0103 \times Vc))$$

$$H3 = \tanh(0.5 \times (-3.2696 + 0.0996 \times ap + 12.3787 \times f + 0.0019 \times Vc))$$

$$H4 = \tanh(0.5 \times (-3.4506 + 2.4092 \times ap - 2.7219 \times f - 0.0034 \times Vc))$$

$$H5 = \tanh(0.5 \times (2.1091 - 0.5186 \times ap + 1.9492 \times f - 0.0041 \times Vc))$$

$$H6 = \tanh(0.5 \times (-6.0975 + 1.7772 \times ap + 12.1907 \times f + 0.0095 \times Vc))$$

$$H7 = \tanh(0.5 \times (4.9372 - 1.8441 \times ap - 6.4098 \times f - 0.0033 \times Vc))$$

$$H8 = \tanh(0.5 \times (-0.0216 + 1.7923 \times ap - 3.9068 \times f - 0.0043 \times Vc))$$

$$H9 = \tanh(0.5 \times (-1.1754 - 0.1424 \times ap + 11.7417 \times f - 0.0077 \times Vc))$$

$$H10 = \tanh(0.5 \times (-4.2862 + 0.4925 \times ap + 21.7649 \times f + 0.0023 \times Vc))$$

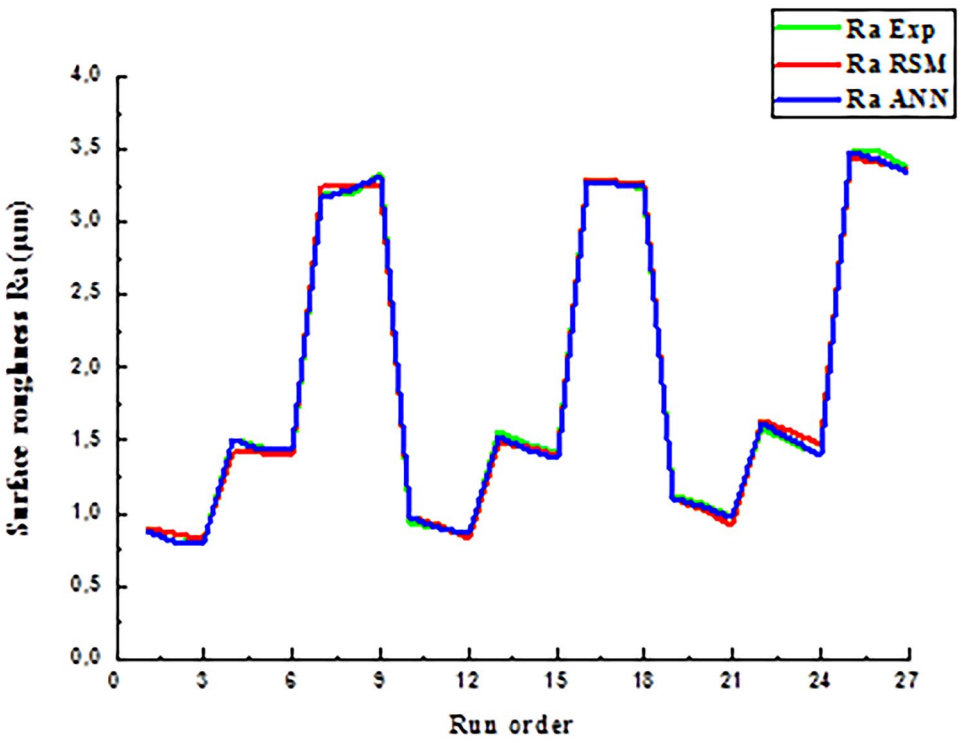

Fig. 10 Experimental, RSM, and ANN predicted results for (*Ra*)

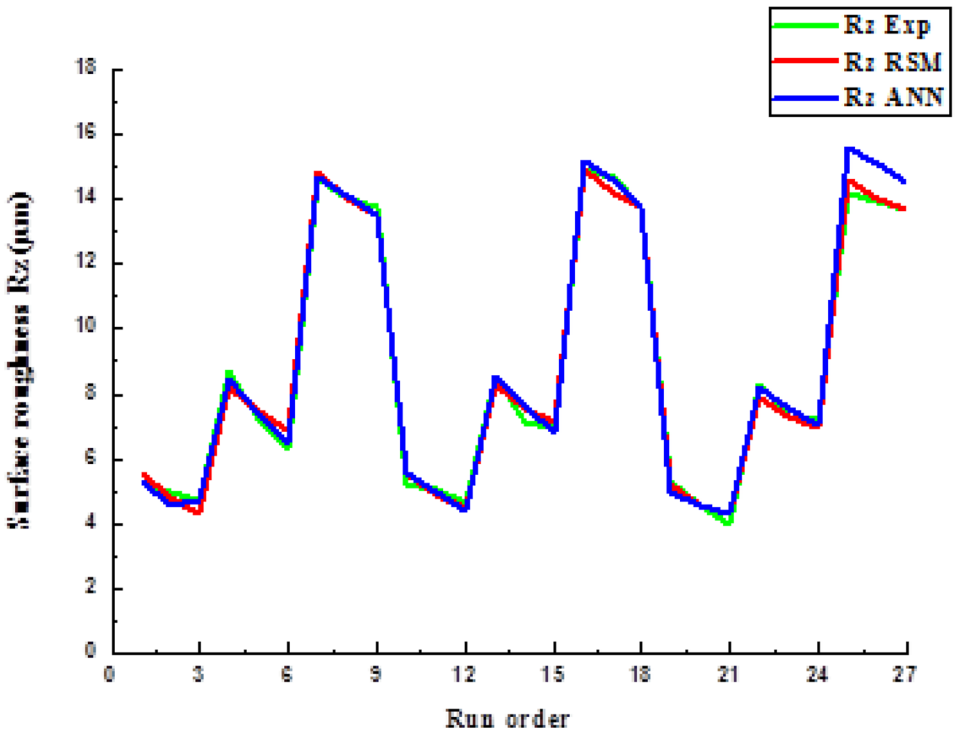

Fig. 11 Experimental, RSM, and ANN predicted results for (*Rz*)

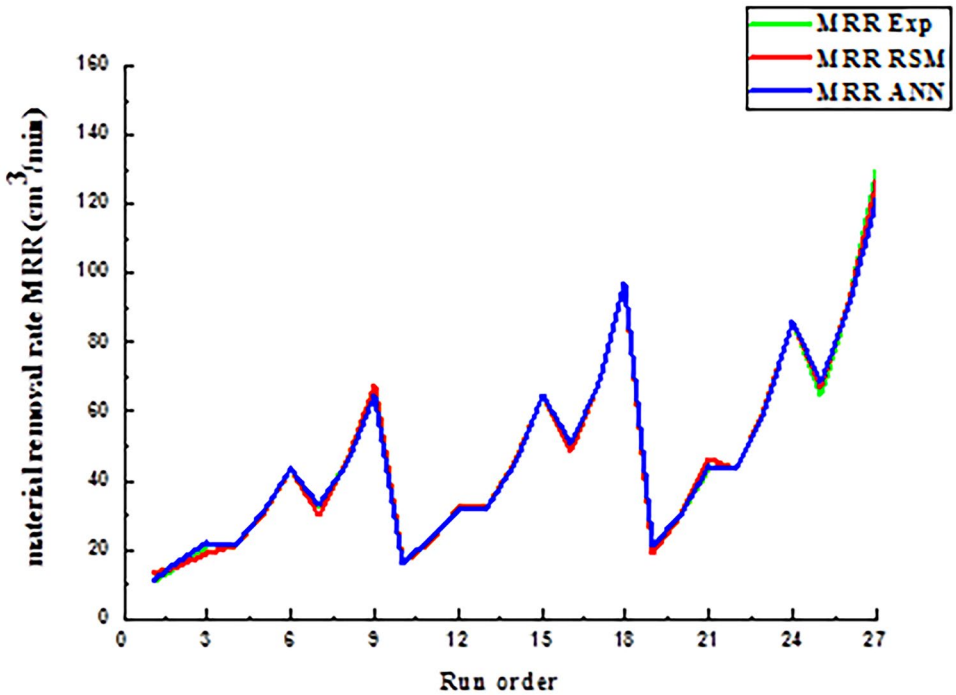

Fig. 12 Experimental, RSM, and ANN predicted results for (*MRR*)

Table 4 Comparison between ANN and RSM prediction results for Ra, Rz, and MRR

Run	Surface roughness (Ra)					Surface roughness (Rz)					Material removal rate (MRR)				
	Exp	Pred. RSM	Pred. ANN	Error (%) RSM	Error (%) ANN	Exp	Pred. RSM	Pred. ANN	Error (%) RSM	Error (%) ANN	Exp	Pred. RSM	Pred. ANN	Error (%) RSM	Error (%) ANN
1	0.89	0.90	0.88	1.12	1.12	5.32	5.57	5.31	4.70	0.19	10.8	13.33	10.65	23.43	1.39
2	0.86	0.87	0.81	1.16	5.81	4.93	4.81	4.55	2.43	7.71	15.2	15.53	16.58	2.17	9.08
3	0.8	0.83	0.79	3.75	1.25	4.72	4.3	4.70	8.90	0.42	21.6	18.73	21.71	13.29	0.51
4	1.51	1.42	1.51	5.96	0	8.7	8.19	8.44	5.86	2.99	21.6	21.6	21.22	0	1.76
5	1.46	1.41	1.44	3.42	1.37	7.19	7.42	7.39	3.20	2.78	30.4	30.4	31.12	0	2.37
6	1.4	1.40	1.44	0	2.86	6.3	6.9	6.47	9.52	2.70	43.2	43.2	43.28	0	0.19
7	3.18	3.24	3.17	1.89	0.31	14.66	14.81	14.71	1.02	0.34	32.4	29.87	32.76	7.81	1.11
8	3.19	3.24	3.23	1.57	1.25	13.99	14.03	14.1	0.29	0.79	45.6	45.27	44.61	0.72	2.17
9	3.34	3.27	3.31	2.10	0.90	13.73	13.5	13.53	1.68	1.46	64.8	67.67	65.13	4.43	0.51
10	0.94	0.97	0.98	3.19	4.26	5.19	5.58	5.54	7.51	6.74	16.2	16.2	16.25	0	0.31
11	0.9	0.91	0.9	1.11	0	5.04	4.89	4.93	2.98	2.18	22.8	22.8	23.37	0	2.50
12	0.84	0.83	0.87	1.19	3.57	4.62	4.48	4.35	3.03	5.84	32.4	32.4	31.77	0	1.94
13	1.56	1.49	1.53	4.49	1.92	8.5	8.25	8.56	2.94	0.71	32.4	32.4	32.3	0	0.31
14	1.48	1.45	1.44	2.03	2.70	7.14	7.55	7.66	5.74	7.28	45.6	45.6	45.26	0	0.75
15	1.42	1.40	1.38	1.41	2.82	6.98	7.13	6.82	2.15	2.29	64.8	64.8	64.72	0	0.12
16	3.3	3.30	3.29	0	0.30	14.92	14.92	15.19	0	1.81	48.6	48.6	50.99	0	4.92
17	3.28	3.28	3.27	0	0.30	14.67	14.21	14.57	3.14	0.68	68.4	68.4	68.85	0	0.66
18	3.22	3.27	3.24	1.55	0.62	13.74	13.79	13.74	0.36	0	97.2	97.2	97.03	0	0.17
19	1.12	1.11	1.1	0.89	1.79	5.29	5.19	5	1.89	5.48	21.6	19.07	21.52	11.71	0.37
20	1.07	1.03	1.04	3.74	2.80	4.58	4.57	4.59	0.22	0.22	30.4	30.07	29.97	1.09	1.41
21	0.98	0.91	0.97	7.14	1.02	3.98	4.27	4.32	7.29	8.54	43.2	46.07	43.83	6.64	1.46
22	1.58	1.64	1.62	3.80	2.53	8.31	7.91	8.17	4.81	1.68	43.2	43.2	43.47	0	0.62
23	1.49	1.57	1.51	5.37	1.34	7.25	7.28	7.56	0.41	4.28	60.8	60.8	60.48	0	0.53
24	1.4	1.48	1.39	5.71	0.71	7.23	6.97	7.03	3.60	2.77	86.4	86.4	86.28	0	0.14
25	3.49	3.45	3.49	1.15	0	14.16	14.62	15.58	3.15	10.03	64.8	67.33	68.62	3.90	5.90
26	3.48	3.41	3.43	2.01	1.44	13.97	13.99	15.1	0.14	8.09	91.2	91.53	90.42	0.36	0.86
27	3.38	3.35	3.33	0.89	1.48	13.71	13.67	14.48	0.29	5.62	129.6	126.73	121.45	2.21	6.29

Table 5 Comparison between RSM and ANN

Measures	Ra		Rz		MRR	
	RSM	ANN	RSM	ANN	RSM	ANN
MAD	0.039	0.024	0.228	0.290	0.848	0.884
MAPE %	2.468	1.647	3.231	3.467	2.880	1.790
R^2	0.9978	0.9992	0.9948	0.9969	0.9973	0.9996

Table 6 Goals and parameters range of optimization for (Ra, Rz, and MRR)

Parameters	Objectives	Lower limit	Upper limit	Importance
Vc (m/min)	Is in range	1	2	3
f (mm/rev)	Is in range	0.08	0.24	3
ap (mm)	Is in range	135	270	3
Ra (µm)	Minimize	0.8	3.49	4
Rz (µm)	Minimize	3.98	14.92	3
MRR (µm)	Maximize	10.8	129.6	3

4.3 Comparison between RSM and ANN models

After ANOVA and modeling, a comparable step between ANN and RSM models was done in terms to improve precision and maximum reliability. Qualified and quantified comparisons are required to evaluate the difference between the experimentally measured values and produced the values and to examine the precision of both models (RSM and ANN) [31]. The constructed model's efficiency was calculated to determine the mean absolute error (MAD), absolute mean percentage error (MAPE), and determination coefficient (R^2). The relationships expressing the different error criteria are given by the Eqs. (17) to (19). The work also concentrated on the accuracy and functionality of the RSM and ANN methods benchmarking approaches. [32, 33].

Figures 10, 11 and 12 illustrate the results that determine the difference between the experimental values and the predicted in the RSM and ANN models for the surface roughness responses and the material removal rate (MRR). Table 4 presents the surface roughness criteria and the material removal rate (MRR), results, predicted by the ANN and RSM models, and the percentage of their absolute errors. The RSM values of the absolute percentage error for (Ra, Rz, and MRR) criteria varied between 0 to 7.14% for Ra, 0 to 8.90%, and 0 to 23.43% for MRR. For the ANN model, they correspond to $Ra = 0$ to 5.81%, $Rz = 0.14$ to 10.03%, and $MRR = 0$ to 9.08%. We conclude that the ANN model provides better results with a low error compared to the RSM model. The obtained values of MAD, MAPE, and R^2 of the response surface methodology (RSM) and the artificial neural network approach (ANN) for Ra, Rz, and MRR are presented in Table 5. Indeed, the ANN model presents the greatest results with the lowest values of MAD and MAPE compared to the RSM model. Consequently, the MAD and MAPE values of the RSM model are 0.039 and 2.468% for Ra, 0.228 and 3.231% for Rz, 0.848 and 2.880% for MRR, respectively. While the ANN model, the values are 0.024 and 1.647% for Ra, 0.290 and 3.467% for Rz, 0.884 and 1.790% for MRR, respectively. Finally, it should be pointed out that all models obtained by the ANN approach have a high determination coefficient ($R^2_{Ra} = 99.92\%$, $R^2_{Rz} = 99.69\%$,

Table 7 Optimization RSM for Ra, Rz, and MRR

	N°	*ap* (mm)	*f* (mm/rev)	*Vc* (m/min)	*Ra* (µm)	*Rz* (µm)	*MRR* (cm^3/min)	***Desirability***
Case 1	1	1.000	0.080	270.000	0.837	4.297	18.733	**0.980**
	2	1.000	0.080	269.463	0.837	4.298	18.714	0.980
	3	1.007	0.080	269.999	0.836	4.303	18.955	0.980
	4	1.000	0.081	269.995	0.836	4.304	19.029	0.980
	5	1.011	0.080	269.992	0.836	4.305	19.048	0.980
Case 2	1	2.000	0.240	270.000	3.355	13.670	126.733	**0.976**
	2	1.996	0.240	270.000	3.354	13.673	126.469	0.976
	3	2.000	0.240	269.317	3.355	13.670	126.432	0.974
	4	2.000	0.239	270.000	3.334	13.600	126.405	0.974
	5	1.994	0.240	270.000	3.354	13.674	126.390	0.973
Case 3	1	2.000	0.126	270.000	1.087	5.345	69.399	**0.743**
	2	2.000	0.126	269.999	1.082	5.321	69.074	0.743
	3	2.000	0.127	270.000	1.093	5.373	69.780	0.743
	4	2.000	0.125	269.998	1.074	5.286	68.603	0.743
	5	2.000	0.128	270.000	1.105	5.425	70.464	0.743

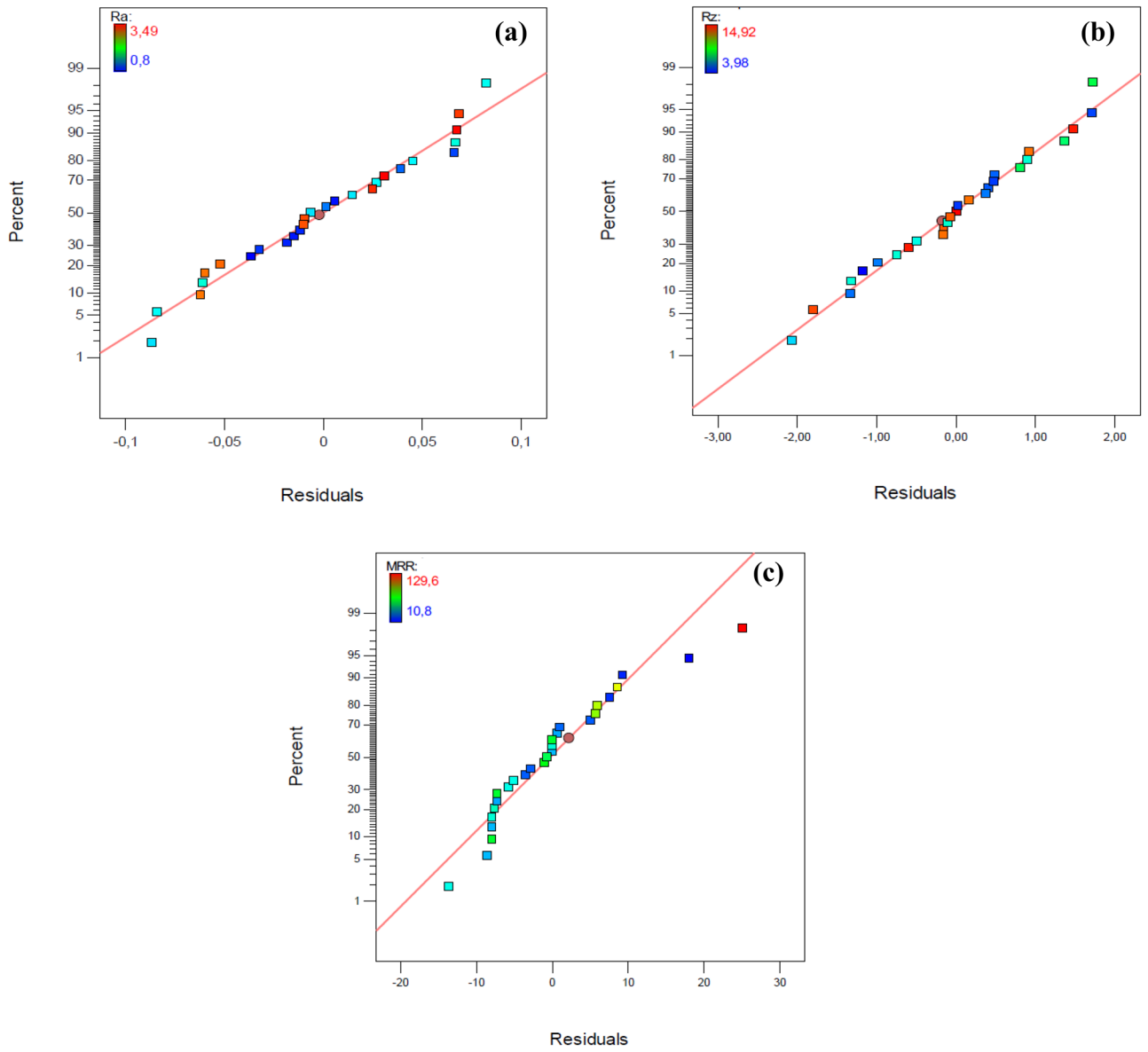

Fig. 13 Normal probability plot of residuals for **a** Ra, **b** Rz, and **c** MRR

and $R^2_{\mathrm{MRR}} = 99.96\%$). The obtained values ($R^2$) of the RSM model for Ra, Rz, and MRR are 99.78, 99.48, and 99.73%, respectively. This can clarify the competence of the ANN model. The deviations in the predicted and experimental results are lower for the ANN model relative to the RSM model; it may be concluded that the ANN model is more adequate for the surface roughness and the material removal rate prediction in the turning of polytetrafluoroethylene.

$$MAPE = \sum_{\mathrm{i}=1}^{\mathrm{n}} \frac{\left|(A_i - B_i)/A_i\right|}{n} \times 100 \tag{17}$$

$$MAD = \sum_{\mathrm{i}=1}^{\mathrm{n}} \frac{\left|A_i - B_i\right|}{n} \tag{18}$$

$$R^2 = \frac{\sum_{i=1}^{n}(B_i - A_i)}{\sum_{i=1}^{n}\left(A_i - Y_e\right)^2} \tag{19}$$

where:

n is the number of experiments.

A_{i} is the experimental value.

B_{i} is the predicted value.

Ye is the average of the experimentally determined values.

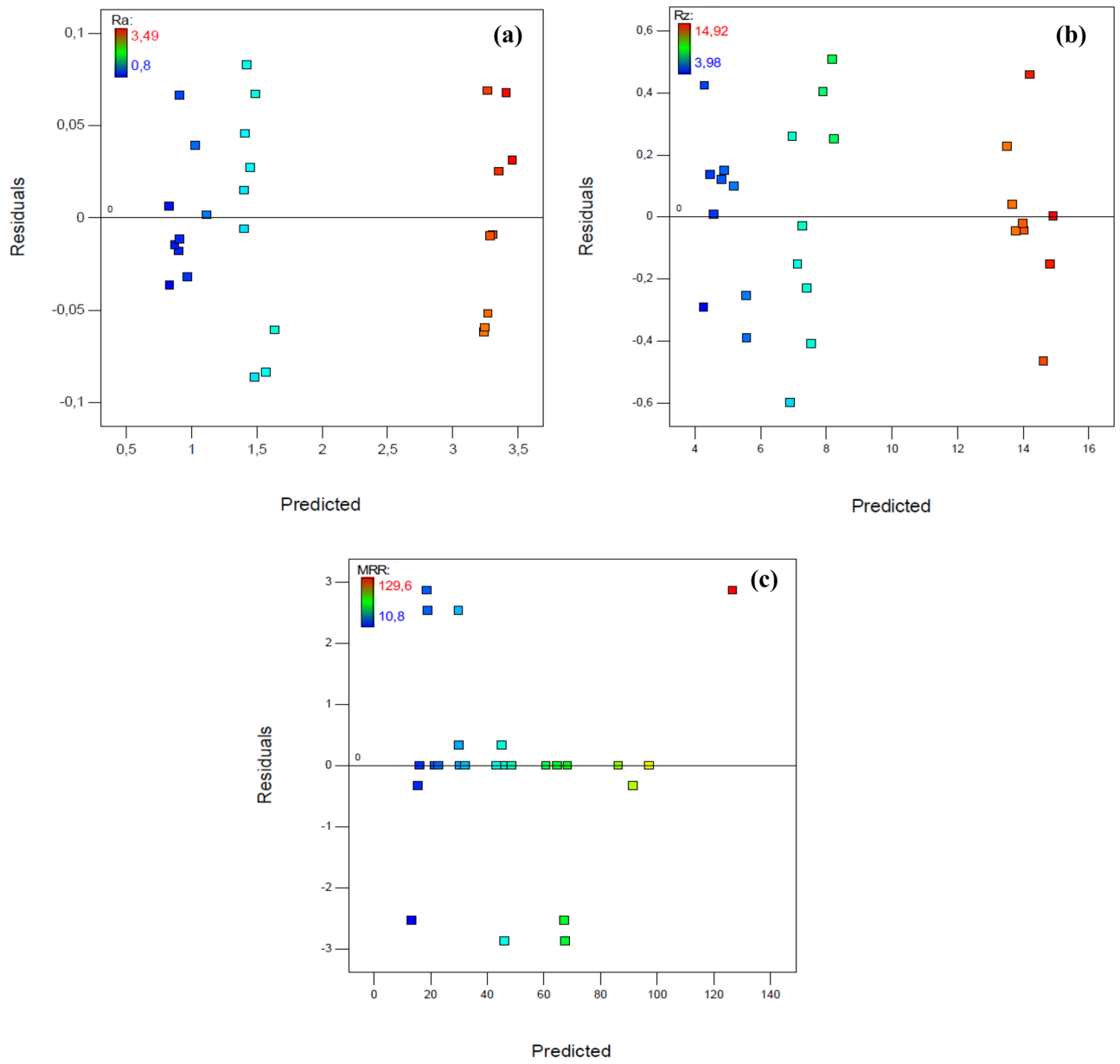

Fig. 14 Residual versus fitted for **a** Ra, **b** Rz, and **c** MRR

4.4 Optimization of responses using the desirability method

The comparison between the experimental values for surface roughness (Ra, Rz) and the material removal rate (MRR) and those estimated by the mathematical models obtained by the RSM and ANN methods is presented in Fig. 9. They found it very close; however, the models obtained by the ANN method confirm a better correlation with the experimental data than those obtained by the RSM method.

Table 6 shows the constraints variation and the range of cutting parameters for the optimization step shown.

Table 7 presents the three solutions selected for the three-optimization cases obtained:

– For case 1, which obtain a good surface quality, the optimal cutting parameters attained are $ap = 1$ mm, $f = 0.08$ mm/rev, and $Vc = 270$ m/min. Surface roughness criteria take a lower value, $Ra = 0.837$ µm and $Rz = 4.297$ µm, while $MRR = 18.733$ cm^3/min and desirability $= 0.98$.

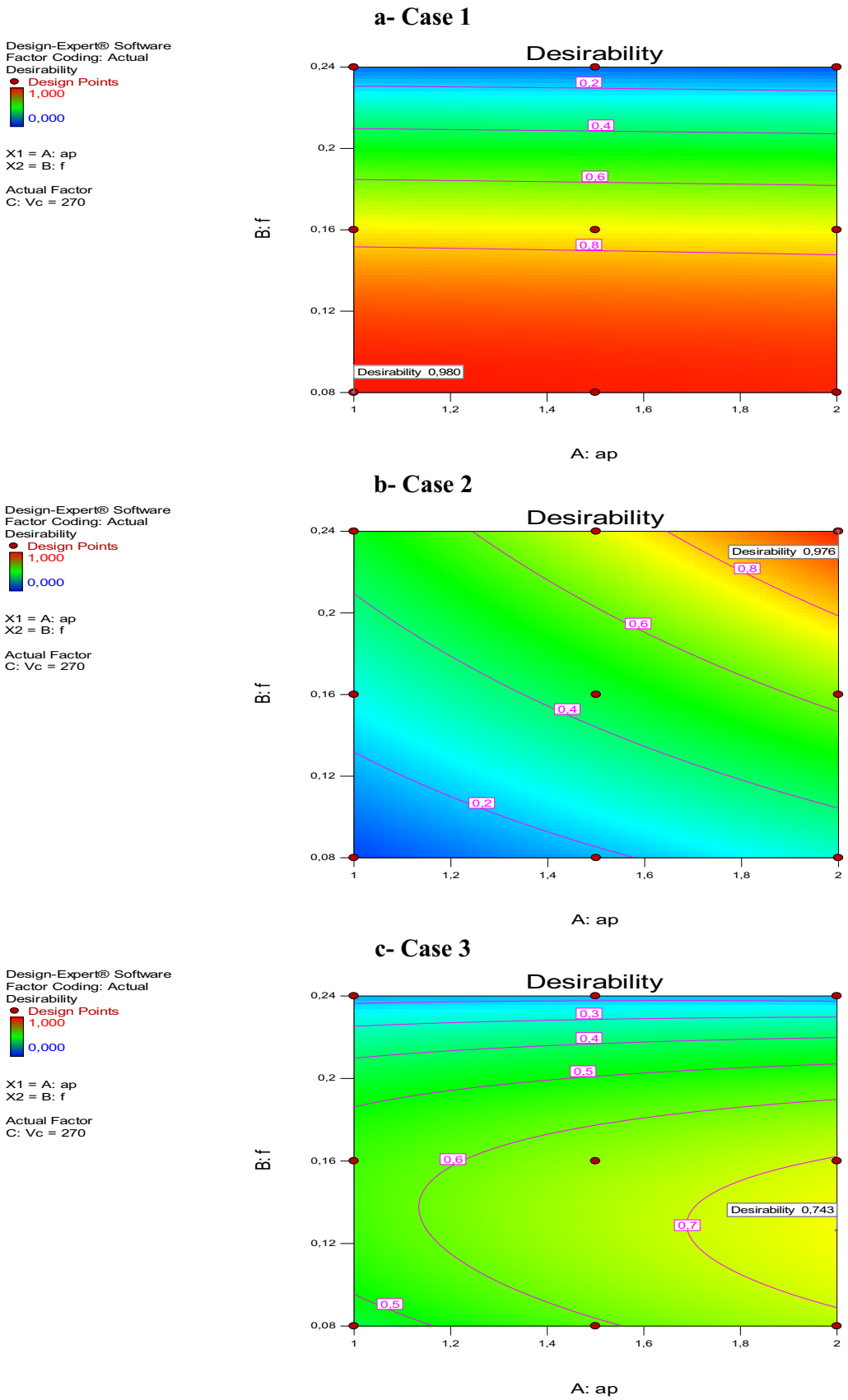

Fig. 15 Contour graphs of desirability for the three-optimization cases

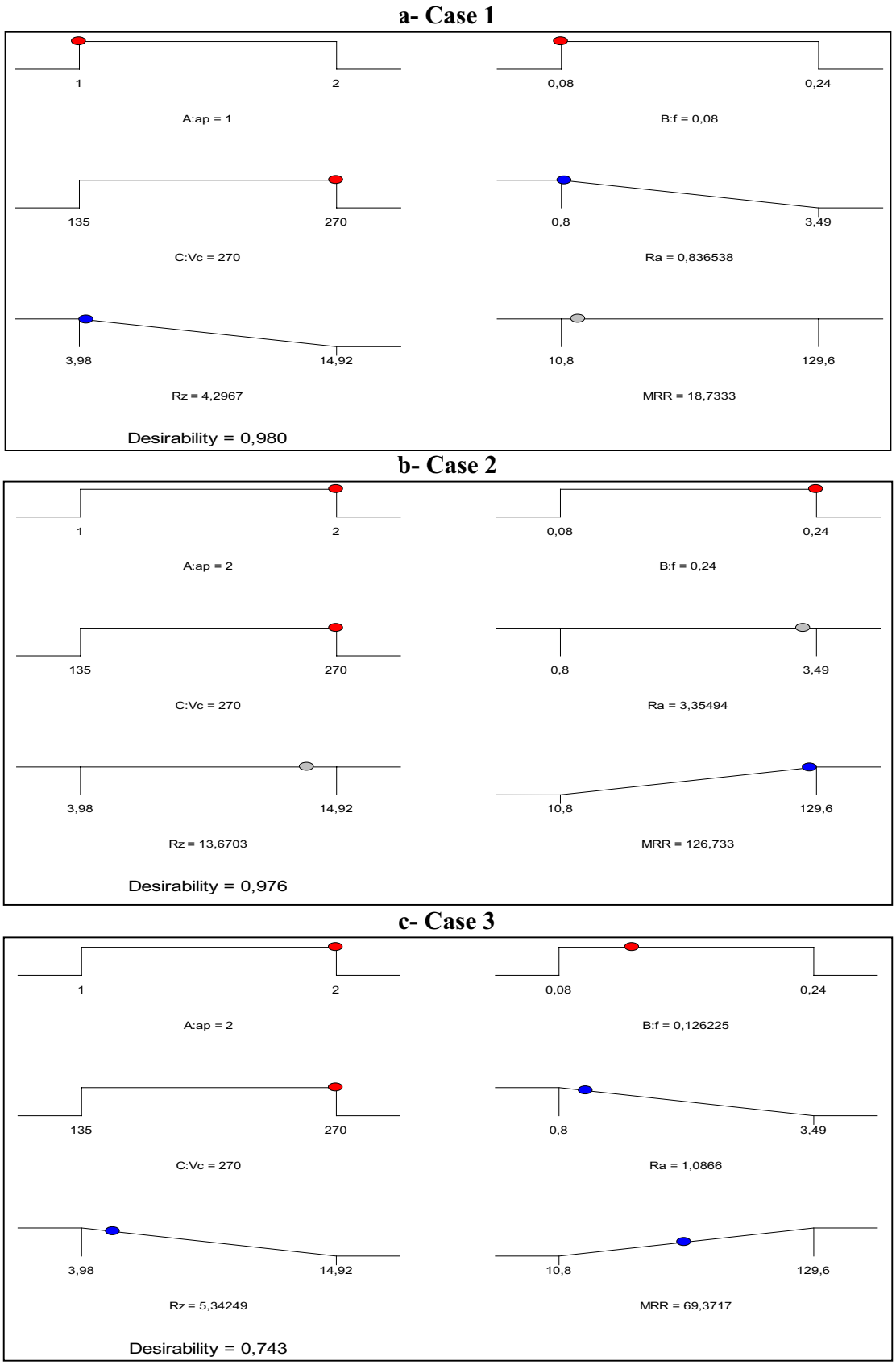

Fig. 16 Ramp function graphs for the three-optimization cases

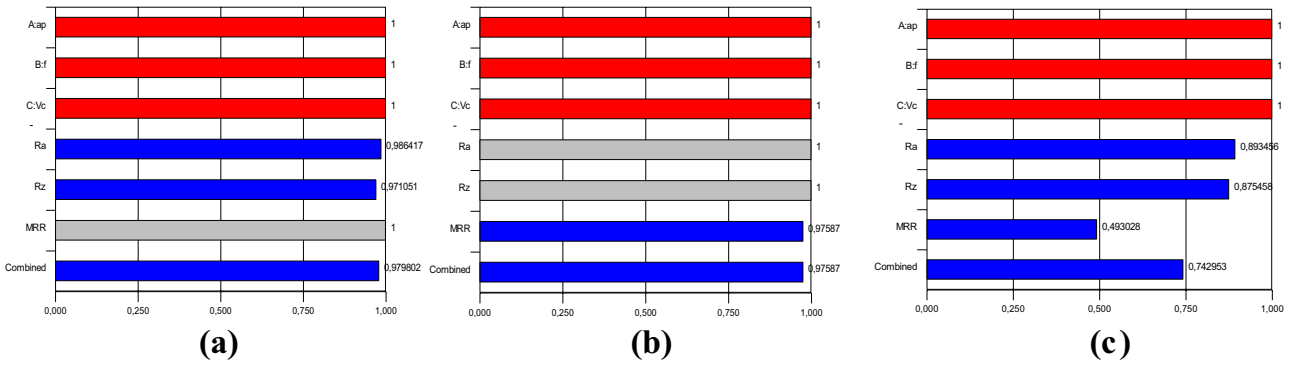

Fig. 17 Bar graphs of desirability for the three-optimization cases, **a** case 1, **b** case 2, and **c** case 3

- For case 2, which obtain the best productivity (MRR) with the optimal cutting parameters, $ap = 2$ mm, $f = 0.240$ mm/rev, and $Vc = 270$ m/min. In this case, the material removal rate takes a maximum value of $MRR = 126.733$ cm^3/min, while $Ra = 3.355$ µm, $Rz = 13.670$ µm, and desirability = 0.976.
- For case 3, which is a combined optimization between (Ra) and (MRR). The optimal cutting parameters obtained in this case are represented by $ap = 2$ mm, $f = 0.126$ mm/rev, and $Vc = 270$ m/min. The minimum roughness and the maximum of the material removal rate reach $Ra = 1.087$ µm, $Rz = 5.345$ µm, and a maximum of $MRR = 69.399$ cm^3/min, while desirability = 0.743.

4.5 Validation of models

The model's suitability shall be verified by the investigations test. Residual analysis is expected to confirm that the ANOVA assumptions are being followed. The difference between the predicted and experimental values is examined, and the residuals versus predicted values are employed. Diagnostic verification was performed by the residual analysis of the developed models. The residual plots are shown in Figs. 13 and 14. It may be seen in Fig. 13a–c the normal probability plots for the output parameter residuals (Ra, Rz, and MRR). The residuals are generally decreased with a straight line, and most of the points are close to the 45° line, indicating that the errors are distributed normally and the proposed model which is significant [34] and can be used to estimate the surface roughness and the material removal rate when turning to polytetrafluoroethylene (PTFE). Residuals versus fitted values should be randomly scattered above and below the zero line, as shown in Fig. 14a–c [35], and this means that the proposed model is adequate.

The industry aims to have better surface quality and high productivity at the same time, a very interesting advantage; this is what we found in the case of the third optimization. Figure 15a–c demonstrates the variation of the desirability as a function of the cutting parameters (*ap*, *f*, and *Vc*) for the various optimization cases along with the contour graphs. The value of desirability is recognized for the three-optimization cases represented by (a) minimization of Ra and Rz, (b) maximum of MRR, and finally (c) a compromise between Ra, Rz, and MRR. Figures 16 and 17 illustrate the desirability ramp plots and the bar graphs for the three-optimization cases.

5 Conclusion

In our work, the modeling and the optimization were presented during the turning of PTFE. Mathematical models for the prediction of roughness criteria (Ra, Rz) and the material removal rate (MRR) as a function of the machining conditions were studied. Based on the outcomes achieved, the following conclusions can be drawn:

1. From the ANOVA, it is proved that the feed rate (*f*) is the most influential parameter on the surface roughness (Ra, Rz) with the contributions of 90.02 and 91.81%, respectively. Moreover, the remaining cutting parameters showed a low significant effect on the surface roughness when turning PTFE.
2. An improvement in surface quality is observed at a lower feed rate and depth of cut with high cutting speed.
3. The material removal rate (MRR) was found affected by the feed rate (*f*) with the contribution of 49.22%, followed by (*ap*, *Vc*) with almost the same contribution of 21.87% and 22%, respectively. The contributions to the interaction process parameter were important.
4. The Pareto chart and the 3D plots confirmed the ANOVA.

5. The correlation coefficients of the predictive models of Ra, Rz, and MRR were found to be about 99.78%, 99.48%, and 99.73%, respectively. Therefore, the developed models are thus accurate and reflect an important industrial interest as they help to make forecasts within the framework of actual experiments.
6. The comparison of the predicted (ANN and RSM) models with the experimental results clearly shows that the ANN models are more reliable and yield excellent results, with high determination coefficient (R^2) and the lowest values of MAD and MAPE compared with the RSM model for surface roughness criteria and the material removal rate:
   - The R^2 values for Ra, Rz, and MRR of the models obtained by ANN present a high determination coefficient of 99.92%, 99.69%, and 99.96%, respectively, while others obtained from the RSM models are 99.78%, 99.48%, and 99.73% for Ra, Rz, and MRR, respectively.
   - The values for the RSM model of MAD and MAPE were obtained as follows: 0.039 and 2.468% for Ra, 0.228 and 3.231% for Rz, and 0.848 and 2.28% for MRR, respectively, while the ANN models are 0.024 and 1.647% for Ra, 0.29 and 3.467% for Rz, and 0.884 and 1.79% for MRR, respectively.
7. The multi-objective optimization of the technological parameters (Ra, Rz, and MRR) using the desirability function (DF) permitted us to find the optimal cutting parameters. Three cases of optimization are recognized in the present study:
   - Case 1: minimization of surface roughness, $ap = 1$ mm, $f = 0.080$ mm/rev, $Vc = 270$ m/min, $Ra = 0.837$ µm, and $Rz = 4.297$ µm
   - Case 2: maximization of the material removal rate, $ap = 2$ mm, $f = 0.240$ mm/rev, $Vc = 270$ m/min, and $MRR = 126.733$ cm^3/min
   - Case 3: compromise between the quality and the productivity, $ap = 2$ mm, $f = 0.126$ mm/rev, $Vc = 270$ m/min, $Ra = 1.087$, $Rz = 5.345$ µm, and $MRR = 69.399$ cm^3/min

Acknowledgements This work was achieved in the Advanced Technologies in Mechanical Production Research Laboratory (LRTAPM), Badji Mokhtar-Annaba University, Algeria. The authors would like to thank the personnel of Mechanics and Structures Research Laboratory (LMS), May 8th, 1945 University, Guelma, for their assistance, as well as the equipment used for the turning of PTFE.

Author contribution I agree.

Availability of data and materials Not applicable.

Code availability Not applicable.

Declarations

Ethics approval As corresponding author, Afef Azzi, I confirm on behalf of all authors that this manuscript has not been published and it's not being submitted to any other journal.

Consent to participate I agree.

Consent for publication I agree.

Competing interests The authors declare no competing interests.

References

1. Rae PJ, Dattelbaum DM (2004) The properties of poly (tetrafluoroethylene) (PTFE) in compression. Polymer 45(22):7615–7625
2. Sanci ME, Halis S, Kaplan Y (2017) Optimization of machining parameters to minimize surface roughness in the turning of carbon-filled and glass fiber-filled polytetrafluoroethylene. Mater Des Appl. Springer, Cham 65:295–305
3. Conesa JA, Font R (2001) Polytetrafluoroethylene decomposition in air and nitrogen. Polym Eng Sci 41(12):2137–2147
4. Huang X, Martinez VJ, Malec D (2014) Morphological evolution of polytetrafluoroethylene in extreme temperature conditions for aerospace applications. J Appl Polym Sci 131(3):39841.1-39841.6
5. Huang X, Martinez VJ, Malec D (2013) Dielectric breakdown and morphological evolution of PTFE during thermal-oxidative ageing at temperatures lower and higher than the melting temperature. Annual Report Conference on Electrical Insulation and Dielectric Phenomena IEEE 148–151
6. DuPont (1996) Fluoroproducts: Teflon PTFE properties handbook: Tech Rep H-37051–3
7. Rooyen LJV, Bissett H, Khoathane MC, Kocsis JK (2016). J Appl Polym Sci. https://doi.org/10.1002/app.43369
8. Raj IJA, Vijayakumar P, Kannan TTM, Pankaj K, Vijayaragavan R (2016) Design optimization of turning parameters of PTFE (Teflon) cylindrical rods using ANOVA methodology. Int J Appl Eng Res 11(3):518–523
9. Sangwan KS, Saxena S, Kant G (2015) Optimization of machining parameters to minimize surface roughness using integrated ANN-GA approach. Procidia CIRP 29:305–310
10. Suresh R, Basavarajappa S, Gaitonde VN, Samuel GL (2012) Machinability investigations on hardened AISI 4340 steel using coated carbide insert. Int J Refract Metal H 33:75–86
11. Mohd SA, Deepak S, Sagar N (2014) Study of cutting forces and surface roughness in turning of bronze filled polytetrafluoroethylene. Int J Adv Mech Eng 4(2):151–160
12. Kaladhar M, Venkata Subbaiah K, Srinivasa Rao CH (2013) Optimization of surface roughness and tool flank wear in turning of AISI 304 austenitic, stainless steel with CVD coated tool. J Eng Sci Technol 8(2):165–176
13. Fetecau C, Stan F (2012) Study of cutting force and surface roughness in the turning of polytetrafluoroethylene composites with a polycrystalline diamond tool. Measurement 45:1367–1379
14. Sanjeev Kumar M, Kaviarasan V, Venkatesan R (2019) Machining parameter optimization of poly tetra fluoro ethylene (PTFE) using genetic algorithm. Int J Modern Eng Res 2(1):143–149
15. Chabbi A, Yallese MA, Meddour I, Nouioua M, Mabrouki T, Girardin F (2017) Predictive modeling and multi-response optimization of technological parameters in turning of polyoxymethylene

polymer (POM C) using RSM and desirability function. Measurement 95:99–115
16. Subramanian M, Kannan TTM, Antony J, Justin Antony raj I (2018) Experimental investigation and optimization of surface roughness on Teflon (PTFE) cylindrical rods using ANOVA methodology. Int Res J Eng Technol 05(5):1943–1947
17. Anand G, Alagumurthi N, Elansezhian R, Palani K, Venkateshwaran N (2018) Investigation of drilling parameters on hybrid polymer composites using grey relational analysis, regression, fuzzy logic, and ANN models. J Braz Soc Mech Sci Eng 40(4):214
18. Azizi MW, Keblouti O, Boulanouar L, Yallese MA (2020) Design optimization in hard turning of E19 alloy steel by analysing surface roughness, tool vibration and productivity. Struct Eng Mech 73(5):501–513
19. Kosky P, Balmer R, Keat W, Wise G (2013) Manufacturing engineering. Exploring Engineering–Elsevier, 205–235
20. Bouzid L, Yallese MA, Belhadi S, Haddad A (2020) Modelling and optimization of machining parameters during hardened steel AISID3 turning using RSM, ANN and DFA techniques: comparative study. J Mech Eng Sci 14(2):6835–6847
21. Kaladhar M (2020) Modeling and optimization for surface roughness and tool flank wear in hard turning of AISI 4340 steel (35 HRC) using Ti Si N-Ti Al N nanolaminate coated insert. Multidiscip Model Mater Struct. https://doi.org/10.1108/MMMS-12-2019-0217
22. Dureja JS, Gupta VK (2010) Design optimization of flank wear and surface roughness for CBN-TiN tools during dry hard turning of hot work die steel. Int J Mach Mach Mater 7(1–2):129–147
23. Asutosh P, Sudhansu Ranjan D, Debabrata D (2019) Statistical analysis of surface roughness using RSM in hard turning of AISI 4340 steel with ceramic tool. Adv Ind Prod Eng 17–26. https://doi.org/10.1007/978-981-13-6412-9_3
24. Ramezani M, Afsari A (2015) Surface roughness and cutting force estimation in the CNC turning using artificial neural networks. Manag Sci Lett 5(4):357–362
25. Paulo DJ, Gaitonde VN, Karnik SR (2008) Investigations into the effect of cutting conditions on surface roughness in turning of free machining steel by ANN models. J Mater Process Technol 205(1–3):16–23
26. Ranganathan S, Senthilvelan T, Sriram G (2010) Evaluation of machining parameters of hot turning of stainless steel (type 316) by applying ANN and RSM. Mater Manuf Process 25(10):1131–1141
27. Tebassi H, Yallese MA, Meddour I, Girardin F, Mabrouki T (2017) On the modeling of surface roughness and cutting force when turning of Inconel 718 using artificial neural network and response surface methodology: accuracy and benefit. Periodica Polytech Mech Eng 61(1):1–11
28. Hagan MT, Demuth HB, Beale MH (1996) Neural network design. PWS Pub. Co, Boston, 3632. Haykin, S (1994). Neural networks: a comprehensive foundation. Prentice Hall PTR
29. Zerti A, Yallese MA, Zerti O, Nouioua M, Khettabi R (2019) Prediction of machining performance using RSM and ANN models in hard turning of martensitic stainless steel AISI 420. Proc Inst Mech Eng C J Mech Eng Sci 233(13):4439–4462
30. Zain AM, Haron H, Qasem SN (2012) Regression and ANN models for estimating minimum value of machining performance. Appl Math Model 36:1477–1492
31. Gupta AK (2010) Predictive modelling of turning operations using response surface methodology, artificial neural networks and support vector regression. Int J Prod Res 48(3, 1):763–778
32. Laouissi A, Yallese MA, Belbah A, Belhadi S, Haddad A (2019) Investigation, modeling, and optimization of cutting parameters in turning of gray cast iron using coated and uncoated silicon nitride ceramic tools. Based on ANN, RSM, and GA optimization. Int J Adv Manuf Technol 101(1–4):523–548
33. Kribes N, Hessainia Z, Yallese MA, Ouelaa O (2012) Statistical analysis of surface roughness by design of experiments in hard turning. Mechanics 18:605–611
34. Montgomery DC (2001) Design and analysis of experiments. John Wiley & Sons Inc, New York
35. Montgomery DC, Runger GC (2003) Applied statistics and probability for engineers, 3rd edn. John Wiley & Sons Inc, USA, p 171